

## Review Article

# Systematic review of computed tomography parameters used for the assessment of subchondral bone in osteoarthritis

Jemima E. Schadow<sup>a</sup>, David Maxey<sup>b</sup>, Toby O. Smith<sup>c</sup>, Mikko A.J. Finnilä<sup>d</sup>, Sarah L. Manske<sup>e</sup>, Neil A. Segal<sup>f</sup>, Andy Kin On Wong<sup>g,h</sup>, Rachel A. Davey<sup>i</sup>, Tom Turmezei<sup>b,j</sup>, Kathryn S. Stok<sup>a,\*</sup>

<sup>a</sup> Department of Biomedical Engineering, The University of Melbourne, Melbourne, Australia

<sup>b</sup> Department of Radiology, Norfolk and Norwich University Hospitals NHS Foundation Trust, Norwich, United Kingdom

<sup>c</sup> Warwick Medical School, University of Warwick, United Kingdom

<sup>d</sup> Research Unit of Health Science and Technology, Faculty of Medicine, University of Oulu, Oulu, Finland

<sup>e</sup> Department of Radiology, McCaig Institute for Bone and Joint Health, Cumming School of Medicine, University of Calgary, Calgary, Canada

<sup>f</sup> Department of Rehabilitation Medicine, The University of Kansas Medical Center, Kansas City, United States

<sup>g</sup> Joint Department of Medical Imaging, University Health Network, Toronto, Canada

<sup>h</sup> Schroeder's Arthritis Institute, Toronto General Hospital Research Institute, University Health Network, Toronto, Canada

<sup>i</sup> Department of Medicine, Austin Health, University of Melbourne, Melbourne, Australia

<sup>j</sup> Norwich Medical School, University of East Anglia, Norwich, United Kingdom

## ARTICLE INFO

## Keywords:

Osteoarthritis  
Computed tomography  
Subchondral bone  
Systematic review

## ABSTRACT

**Objective:** To systematically review the published parameters for the assessment of subchondral bone in human osteoarthritis (OA) using computed tomography (CT) and gain an overview of current practices and standards. **Design:** A literature search of Medline, Embase and Cochrane Library databases was performed with search strategies tailored to each database (search from 2010 to January 2023). The search results were screened independently by two reviewers against pre-determined inclusion and exclusion criteria. Studies were deemed eligible if conducted *in vivo/ex vivo* in human adults (>18 years) using any type of CT to assess subchondral bone in OA. Extracted data from eligible studies were compiled in a qualitative summary and formal narrative synthesis.

**Results:** This analysis included 202 studies. Four groups of CT modalities were identified to have been used for subchondral bone assessment in OA across nine anatomical locations. Subchondral bone parameters measuring similar features of OA were combined in six categories: (i) microstructure, (ii) bone adaptation, (iii) gross morphology (iv) mineralisation, (v) joint space, and (vi) mechanical properties.

**Conclusions:** Clinically meaningful parameter categories were identified as well as categories with the potential to become relevant in the clinical field. Furthermore, we stress the importance of quantification of parameters to improve their sensitivity and reliability for the evaluation of OA disease progression and the need for standardised measurement methods to improve their clinical value.

## 1. Introduction

Osteoarthritis (OA) is a disease affecting the whole joint, where bone plays an important role in the pathology. Subchondral sclerosis, osteophytes and cysts are recognised osseous features of OA that arise in early stages of disease [1–3]. Furthermore, studies have demonstrated that

abnormal bone remodelling may be a precursor of cartilage degradation [4–6].

Computed tomography (CT) is an imaging technique with three-dimensional (3-D) reconstruction capabilities that employs X-ray to visualize the internal structure of an object of interest. Whilst it is not the only 3-D imaging modality available, its ability to image bone at high

\* Corresponding author at: Department of Biomedical Engineering, University of Melbourne, Biomedical Engineering Building 261, Parkville, Victoria 3010, Australia.

E-mail addresses: [jeschadow@student.unimelb.edu.au](mailto:jeschadow@student.unimelb.edu.au) (J.E. Schadow), [david.maxey@doctors.org.uk](mailto:david.maxey@doctors.org.uk) (D. Maxey), [toby.o.smith@warwick.ac.uk](mailto:toby.o.smith@warwick.ac.uk) (T.O. Smith), [mikko.finnila@oulu.fi](mailto:mikko.finnila@oulu.fi) (M.A.J. Finnilä), [smanske@ucalgary.ca](mailto:smanske@ucalgary.ca) (S.L. Manske), [nsegal@kumc.edu](mailto:nsegal@kumc.edu) (N.A. Segal), [andy.wong@uhnresearch.ca](mailto:andy.wong@uhnresearch.ca) (A.K.O. Wong), [r.davey@unimelb.edu.au](mailto:r.davey@unimelb.edu.au) (R.A. Davey), [tom.turmezei@nnuh.nhs.uk](mailto:tom.turmezei@nnuh.nhs.uk) (T. Turmezei), [kstok@unimelb.edu.au](mailto:kstok@unimelb.edu.au) (K.S. Stok).

<https://doi.org/10.1016/j.bone.2023.116948>

Received 15 August 2023; Received in revised form 4 October 2023; Accepted 19 October 2023

Available online 3 November 2023

8756-3282/© 2023 The Author(s). Published by Elsevier Inc. This is an open access article under the CC BY-NC-ND license (<http://creativecommons.org/licenses/by-nc-nd/4.0/>).

resolution with standardised segmentation protocols is currently unsurpassed [7,8]. The technology can be adapted for various applications from clinical imaging to experimental tissue level characterisation. Micro-CT achieves resolutions on the micro-scale, but with high radiation dose and limited sample size mainly suitable for tissue samples, biopsies and small animal studies [9]. Multidetector CT with helical (also sometimes called “spiral”) acquisition uses specialised detector arrays to reduce noise, improve resolution and reduce scanning times for subjects *in vivo* [10]. Cone-beam CT technology uses x-rays in the shape of a cone rather than a fan, as in multidetector CT. While this has a lower dose than conventional CT, maintaining resolution at this lower radiation dose comes at the cost of increased noise and poorer contrast resolution [11].

Currently plain film/digital radiography and magnetic resonance imaging (MRI) are deemed the imaging modalities of choice for OA assessment [1,12–14]. Plain film and digital radiography are standardly used for imaging of structural bone changes and joint space narrowing for OA diagnosis and disease severity assessment [1,15]. The two-dimensional images allow for general assessments of bony structures but do not depict soft tissue, lack sensitivity to disease progression and local differences and are prone to positioning and image acquisition reproducibility issues [15–17]. MRI has been shown to be a valuable tool for soft tissue imaging, capturing changes of cartilage, ligaments, menisci, and synovium, as well as bone marrow oedemas [12,14]. CT has advantages over both methods in the assessment of mineralised structures, especially bone. In particular, the capability to deliver higher resolution 3-D image reconstructions enables greater standardisation in analysis of bone structures compared to other imaging modalities [18,19]. Conventional clinical CT scanners typically have a spatial resolution of 240  $\mu\text{m}$  (Supplementary Table 15) [20–22] whereas 3 T MRI scanners usually achieve a spatial resolution of 500–700  $\mu\text{m}$ , depending on the acquisition protocol used [23]. More advanced CT technologies, such as high-resolution peripheral quantitative CT (HR-pQCT) and photon-counting CT achieve spatial resolutions of 58–110  $\mu\text{m}$  (Supplementary Table 15) [24,25] capable of imaging bone microstructure using standardised acquisition and image processing protocols. Pre-clinical research has shown that additionally to larger structural changes, microstructure significantly changes in OA [26]. With a growing understanding of the importance of bone in OA pathology, we consider it an important juncture to recognise the opportunities that CT holds in the imaging assessment of OA [27]. In this study, we systematically review categories of published parameters for the assessment of subchondral bone in human OA using CT to gain a general overview of current practices and standards.

## 2. Methods

### 2.1. Protocol and registration

This systematic review followed a predetermined protocol and has been reported in accordance with the PRISMA 2020 statement [28]. The protocol was registered with PROSPERO, registration number CRD42021271530.

### 2.2. Search strategy and study selection

An electronic search of MEDLINE, EMBASE, and Cochrane Library databases was performed, each with a search strategy tailored to match their syntax. The search was limited from 2010 to September 2021, due to the limited application of CT in the context of OA before this time-frame. A full description of the search strategy used is recorded in Supplementary Tables 1–3. Because of the long duration between the first search and the publication, an additional secondary electronic search of the same databases from September 2021 to January 2023 was performed using the same search terms.

### 2.3. Eligibility criteria

Papers that met the following criteria were included in the review: (1) conducted *in vivo/ex vivo* in human adults (age  $\geq 18$  years old); (2) using any type of CT technology for the study; (3) studying subchondral bone, in synovial joints; (4) written in the English language; (5) having full-text paper available to authors; (6) not investigating pre-operative arthroplasty planning; (7) not investigating post-arthroplasty imaging; and (8) published from 2010. Criteria (6) and (7) aimed to focus the search on subchondral bone, as pre-operative arthroplasty planning and post-arthroplasty imaging mostly do not involve subchondral bone analysis. The titles and abstracts of the studies were independently screened by two reviewers (JES, DM). The full text of potential studies was screened against the inclusion criteria for the final selection independently by the same reviewers. Any disagreements that arose during screening were resolved by a third reviewer (TT).

### 2.4. Data extraction

The following data were extracted from included studies: (1) patient demographics (age, sex, body mass index (BMI)); (2) CT specifications (type, make, model, scan parameters); (3) joint examined; (4) details of joint positioning; (5) load-bearing status; (6) contrast agent details (use, route of administration, dose); (7) image processing methods (reconstruction parameters, post-processing analysis technique); (8) region of interest range and anatomical reference(s); (9) data type (quantitative/semi-quantitative/qualitative); (10) OA classification; (11) array of juxta-articular radiographic subchondral bone features described; (12) any predictors/correlates of the subchondral bone features measured; (13) simultaneous soft tissue assessment; (14) any clinical outcome predicted by/correlated with the measured subchondral bone features; (15) description of complications arisen from OA (e.g. osteonecrosis, chondrolysis, stress fractures); and (16) the use of any comparator modality. The data was extracted by one reviewer (JES) and, as per standard practice, randomly selected 10 % of all extracted data was independently verified by a second reviewer (DM) [29]. Disagreements were resolved by a third reviewer (TT).

### 2.5. Quality assessment

A standardised quality scoring tool, Newcastle-Ottawa scale, developed by the Ottawa Hospital Research Institute was used to assess the scientific quality of case-control and cohort studies and a modified Newcastle-Ottawa scale adapted for cross-sectional studies was used for the quality assessment of cross-sectional studies (Supplementary Material Tables 4–6) [30]. The tool comprises eight questions that evaluate study group selection, their comparability, and ascertainment of outcome or exposure of the respective study. The study designs were confirmed and subsequently the quality assessment was completed by one reviewer (JES). Ten percent of all quality assessments were independently verified by a second reviewer (DM). Disagreements were resolved by a third reviewer (TT).

### 2.6. Data synthesis

A meta-analysis was considered inappropriate for this study as the research question aimed to assess the frequency of reported CT parameters, rather than exploring comparisons or relationships requiring formal statistical testing. Therefore, a qualitative summary and formal narrative synthesis of the results were compiled to report findings of the review.

### 3. Results

#### 3.1. Study selection

The results of the search strategy are summarised in Fig. 1. In total, 8813 papers were identified by the initial search across all databases of which 2280 duplicates were removed. The resulting 6533 papers were screened for title and abstract of which 6190 papers were excluded. The remaining 346 full-text articles were retrieved, of which three were irretrievable. After the full-text assessment, 246 were found to be relevant. Among these, 21 did not specify the age of their participants and 23 included a small number of participants younger than 18 years and were, as per exclusion criteria, further excluded from analysis. The latter were not excluded earlier in the screening process as the majority of participants included in these studies were adults and it was only following detailed screening of the full-text articles that select participants under 18 years included in those studies were identified. Finally, 202 full-text papers were included in the analysis.

#### 3.2. Quality assessment

Scores were separately assessed for cross-sectional, cohort and case-control studies. Detailed score and scoring items can be found in Supplementary Material Tables 4–9. Quality scores were calculated as a percentage of the total score (nine points; selection: four, comparability: two, exposure: three). The mean quality scores (range) of 188 cross-sectional studies, 11 cohort studies and three case-control study were 51 % (0–89), 66 % (33–89) and 63 % (56–67) respectively. Little mean quality differences were observed between different categories, CT groups and anatomical location (Supplementary Fig. 1).

#### 3.3. Study characteristics

Table 1 categorises CT modalities reported in the included studies in four groups; conventional clinical-type CT, quantitative CT for human use, micro-/nano-CT and cone-beam CT. Study characteristics are summarised in Table 2. Four reports used more than one CT type for

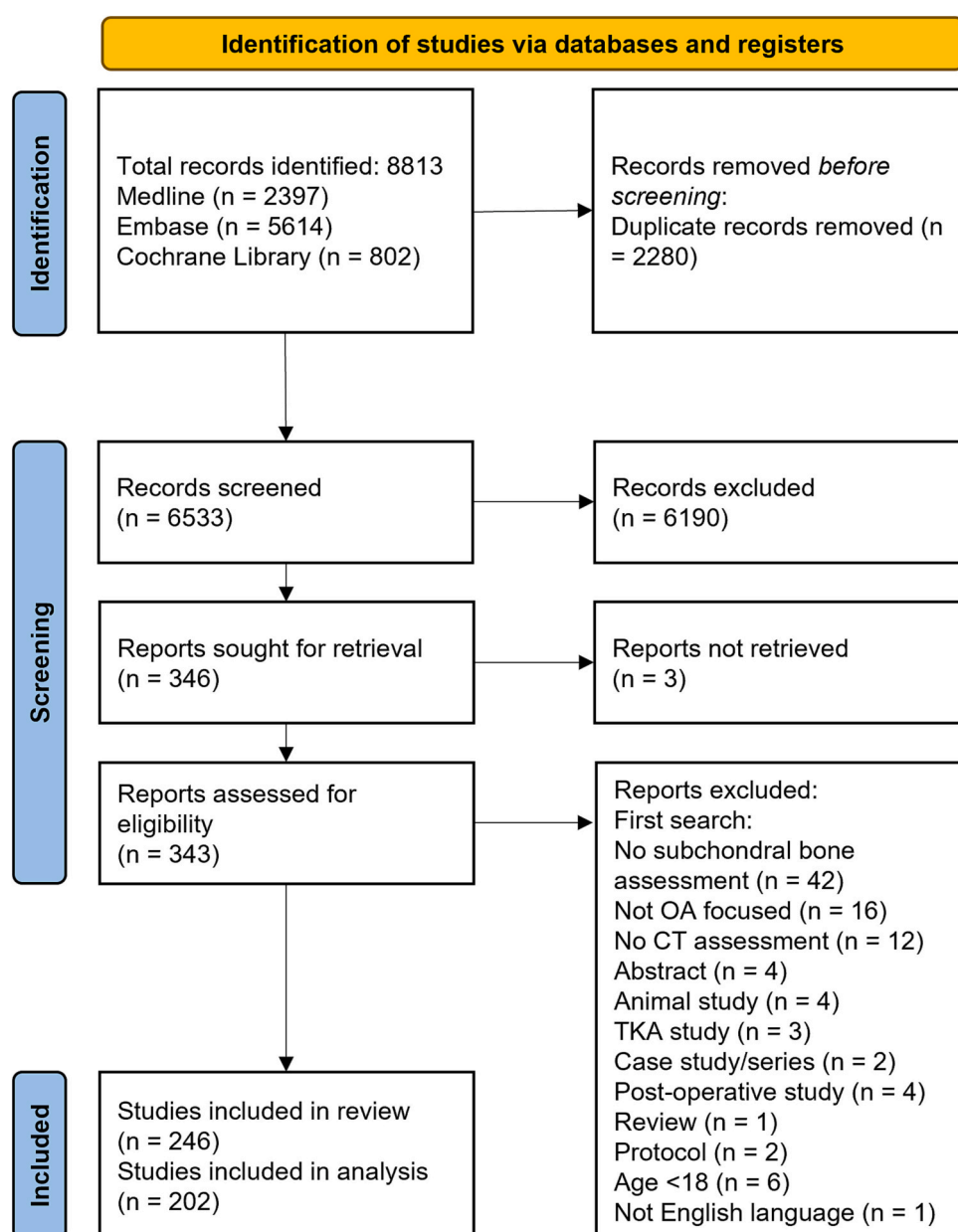


Fig. 1. PRISMA flow diagram of study selection.

**Table 1**  
Description of CT modalities included in each CT group defined and a brief explanation of each group.

CT group	CT modalities included	Explanation
Conventional clinical-type CT	Multidetector CT	Fan-beam CT technologies conventionally used for radiological assessment
	Spiral CT	
	Positron emission/CT	
	Four-dimensional CT	
Quantitative CT for human use	Thin-slice CT	CT technologies (QCT: fan-beam, HR-pQCT: cone-beam) usually including a density phantom during imaging commonly used for quantitative bone mineral density assessment in humans
	Quantitative CT (QCT)	
	HR-pQCT	
Micro-/ nano-CT	MicroCT	Fan-beam CT technologies capable of micro-/ nano-scale resolution, commonly used for <i>ex vivo</i> / pre-clinical <i>in vivo</i> investigations
	Synchrotron radiation CT	
Cone-beam CT	Cone-beam CT (CBCT)	Cone-beam CT technologies commonly used for dental/ maxillofacial and upper/ lower limb assessment (CBCT) and <i>ex vivo</i> / pre-clinical <i>in vivo</i> investigations (CBmicroCT)
	Cone-beam microCT	
	(CBmicroCT)	

**Table 2**  
CT groups, anatomical locations, parameter categories and their corresponding references and reporting frequencies.

Subject		References	Reporting frequency
CT group	Micro-/ nano-CT	[31,33,34,58,63–129]	71
	Conventional clinical-type CT	[31,32,34,57,60,62,130–187]	64
	Cone-beam CT	[33,188–220]	34
	Quantitative CT for human use	[31,59,61,221–232]	15
Anatomical location	Knee	[31–34,42,48,53,62–66,73–80,82–86,94,95,97,99,100,102–108,110,114,115,122,125,126,139,146,148,156,166,170,171,178,179,182,184,203,209–211,220–228,232]	70
	Hip	[32,41,45,67–72,89–92,96,101,109,111–113,116–121,123,127–129,133,137,158,160,176,177,229,230,233]	38
	Wrist/ Hand	[46,50,58–61,87,88,93,132,138,150,151,163,183,231]	28
	Temporomandibular joint	[172,181,188–199,201,202,204–208,213–216,219]	26
	Shoulder	[32,35–40,43,44,47,51,52,54–56,124,131,135,136,142,143,162,174,186]	24
	Spine	[32,49,57,98,130,140,141,144,145,149,152–155,168,169,187]	19
	Ankle/ Foot	[32,81,147,159,164,165,167,173,175,180,185,200,212,217,218]	15
	Elbow	[161]	1
	Sacroiliac joint	[134]	1
	Category		
	Microstructure	[33,34,47,48,59,61,63–78,80–98,100–112,114–129,137,138,147,159,181,182,189,199,202,204,206,209,210,213,221,226,228–230,232]	90
	Bone adaptation	[31,41,46,48,50,57,58,60,61,65,109,118,120,121,125,127,133,134,138,139,142,143,146,158,159,161,163,165,166,172,173,181,183–185,187,189–192,194,196,197,199,201,202,204,205,208,211,214,216,218,222,229,231,233]	57
	Gross morphology	[35–40,42,44,50,53–56,60,61,69,113,131,132,135,136,143,147,150,152,159,165,171,175,177–181,183,186,189–196,198–201,205,207,208,214,217,219]	54
	Mineralisation	[47,48,59,61,64–66,69,72,74,75,78,79,87,89–92,100,103,115–118,120,121,124,126,127,142,146,148,151,160,164,167,170,176,181,182,186,199,203,206,223–227,230,232,234]	52
	OA classification	[32,43,45,49,51,52,62,99,130,131,140,141,144,145,149,153–155,162,168,169,174,193,212,215]	25
	Joint space	[35,50,57,60,134,137,158,165–167,172,199,220,222,233]	15
	Mechanical properties	[61,63,68,82,114,124,127,176,221]	9

their study [31–34] and 22 papers did not specify what type of CT technology was used, whereby no assumption could be made [35–56]. Furthermore, eight papers investigated more than one joint [32,50,57–62]. Of these, one study investigated multiple joints in the neck [57], five studies investigated multiple joints in the hand [50,58–61], one study investigated multiple articulations within the knee [62], and one study investigated joints in the neck, shoulder, hip, knee, and ankle as well as two facet joints each of the lumbar, thoracic and cervical spine [32].

Study participants of the included studies were males and females of at least 18 years old. They either suffered from OA, were at risk of suffering from OA or served as control groups. Whilst studies focussing on pre-arthroplasty planning and post-arthroplasty imaging were excluded, studies using pre-arthroplasty images for alternative analysis were included. Furthermore, samples retrieved for micro-/nano-CT imaging were retrieved from patients undergoing arthroplasty or from body donors.

Subchondral bone parameters assessed with CT technology were categorised into six subgroups as reported across the included studies. Parameters measuring similar features of OA were combined in

categories and defined as: (i) microstructure; (ii) bone adaptation; (iii) gross morphology; (iv) mineralisation; (v) joint space; and (vi) mechanical properties. Twenty-five studies did not generate any subchondral bone parameters using segmentations but semi-quantitatively or qualitatively graded OA severity by visual inspection of CT images.

3.4. Microstructure

Microstructural parameters included parameters such as trabecular and cortical thickness, porosity, trabecular separation or trabecular plate to rod ratio that assess the microarchitecture and were investigated in 30 % of the included studies (Table 2, Fig. 2). Microstructural parameters were predominantly measured at the hip (41 %) and knee joints (39 %). Of all measurements, 81 % were acquired *ex vivo* with micro-/ nano-CT technology (Fig. 3). Illustrated in Fig. 4, reported microstructural parameters were almost exclusively quantitative (98 %) with the exception of porosity (perforations/channels) [78] and bone thickness (cortical thickness) [204] that were analysed qualitatively in one study each.

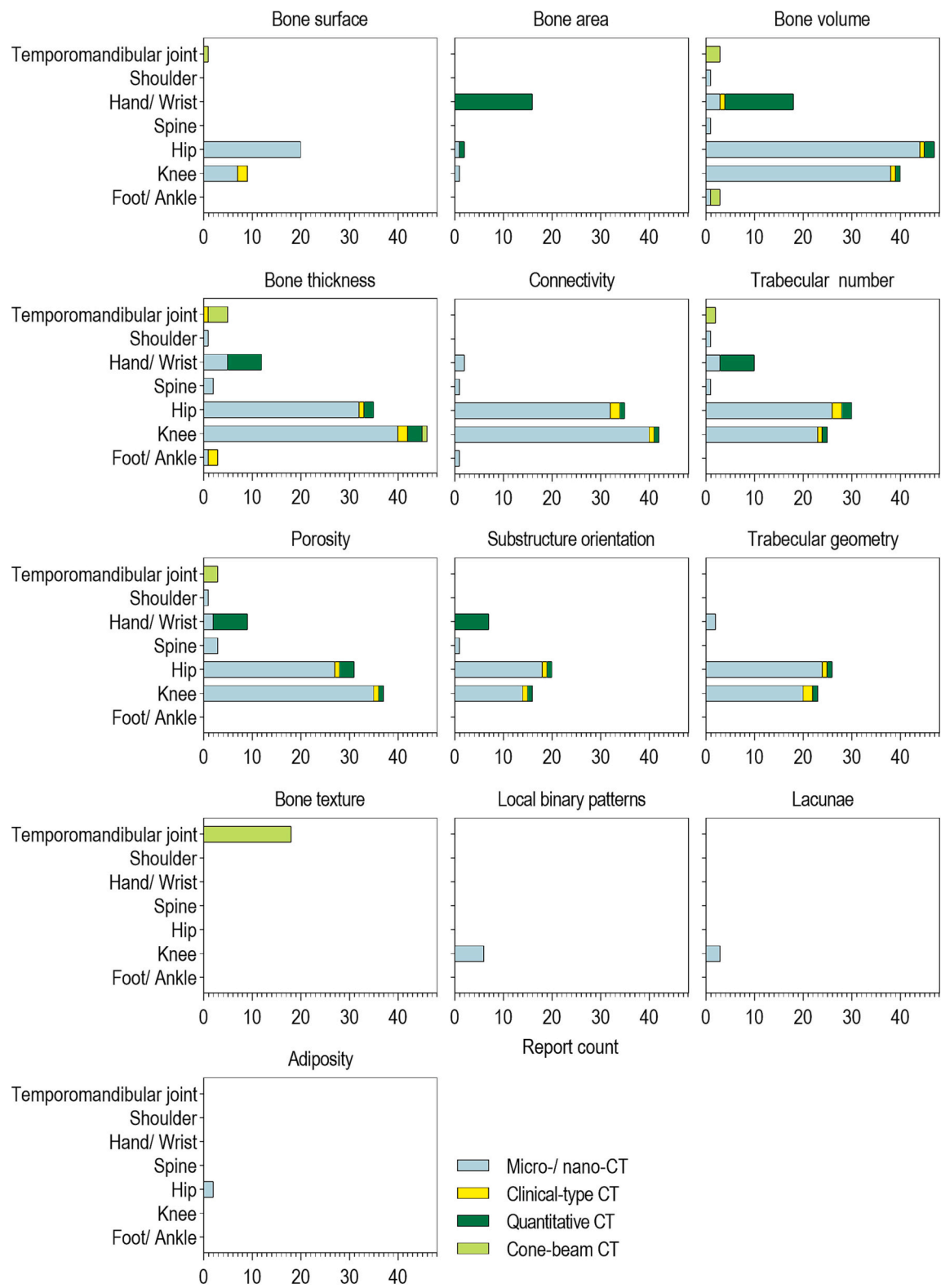


**Fig. 2.** Report count of quantitative parameters measuring microstructure features in the respective anatomical location and distribution of CT technology used for measurement. Two qualitative parameters (Perforations/ channels: knee, micro-/nano-CT; Cortical thickness: TMJ, cone-beam CT) are not included in the fig. A detailed description of parameters can be found in Supplementary Materials Table 10.

3.5. Bone adaptation

Bone adaptation parameters included those indicative of abnormal bone remodelling in the context of osteoarthritis, such as the presence of osteophytes, cysts, erosion, or sclerosis as well as measures of bone

alteration over time, which were reported in 19 % of all studies (Table 2, Fig. 5). Studies reporting bone adaptation most frequently employed clinical-type CT (45 %) and cone-beam CT (32 %) technology. Cone-beam CT was nearly exclusively used to investigate temporo-mandibular joints (TMJ) [189–192,194,196,197,199,201,202,204,205,



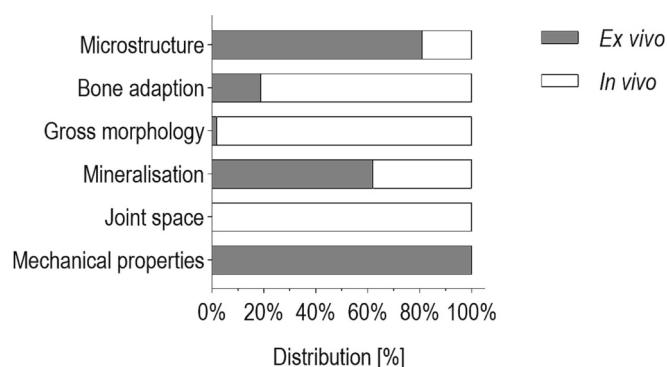


Fig. 3. Distribution of *ex vivo* and *in vivo* imaging in each category.

208,214,216] except for two studies that used it to investigate ankle [218] and knee joints [211], whereas conventional clinical-type CT was used to study joints across all anatomical locations. Qualitative parameters such as the presence or absence of osteophytes or subchondral cysts made up 42 % of all bone adaptation parameters. The remaining half was made up of 35 % quantitative and 23 % semi-quantitative parameters (Fig. 4).

### 3.6. Gross morphology

This category encompassed parameters describing alignment and the shape of bone such as bone surface areas, alignment angles or bone flattening. Illustrated in Table 2, 18 % of studies investigated gross morphology. A variety of parameters in many anatomical locations were recorded (Supplementary Fig. 2). Gross morphological parameters were used to describe TMJ (27 %), foot/ankle (21 %), shoulder (17 %), knee (13 %), hand/wrist (12 %), hip (10 %) and spinal joints (<1 %). Clinical-type CT (50 %) and cone-beam CT (43 %) were the dominant technology used. Parameters describing gross morphology were 60 % quantitative, 28 % qualitative and 12 % semi-quantitative (Fig. 4).

### 3.7. Mineralisation

Mineralisation included parameters describing tissue mineralisation such as bone mineral density, tissue mineral density and attenuation values, which were analysed in 17 % of studies (Table 2, Fig. 6a). Micro-/nano-CT was used in 50 % of studies and the main anatomical locations of interest were knee (51 %), wrist/hand (19 %) and hip joints (18 %). Three reports of qualitative parameters were recorded (high-density mineralised protrusions attenuation [146], subchondral bone plate attenuation [146], free calcifications [199]), however the other 96 % were quantitative (Fig. 4).

### 3.8. Joint space

Joint space parameters described the space between the bony articular surfaces at the joint and were reported in 5 % of studies (Table 2, Supplementary Fig. 3). Clinical-type CT was used to determine joint space parameters in 79 % of cases across various anatomical locations. The distribution of quantitative, semi-quantitative, and qualitative parameters was 36 %, 50 % and 14 %, respectively (Fig. 4).

### 3.9. Mechanical properties

Estimated mechanical properties such as tissue stiffness and failure load were reported in 3 % of studies (Table 2, Fig. 6b). These parameters were indirectly derived from finite element analysis techniques that were based on images obtained with all CT types, with the exception of one study that utilised CT image-guided mechanical evaluation [124]. Mechanical properties were derived for wrist/ hand (40 %), hip (27 %),

knee (20 %), and shoulder joints (13 %) which were exclusively quantitative in nature (4).

## 4. Discussion

This systematic review summarises published CT parameters describing subchondral bone measurements in humans with OA. We have devised appropriate categories encompassing these parameters and stratified them according to CT technology applied and the joints which were investigated. Here we summarise the narratives from these six major parameter categories, specifically microstructure, adaptation, gross morphology, mineralisation, joint space, and mechanical properties.

### 4.1. Microstructure – bench to bedside

Microstructural parameters were mainly analysed in studies analysing OA pathogenesis and characterising and phenotyping OA. They are considered useful to investigate the connections of different tissue changes as well as the influence of risk factors, resulting in indications for new disease biomarkers. Microstructure was also the subject of method development and validation studies, investigating the sensitivity and ability of novel methods to image microstructure. Micro-/nano-CT was the most frequently used technology for the analysis of bone microstructure, mainly in knee and hip joints. It can capture high-resolution images with spatial resolution down to 200 nm (Supplementary Table 15) [235,236], thus enabling quantitative assessment of trabecular architecture measuring features like trabecular thickness, trabecular number and cortical porosity. However, the radiation dose is too high and gantry size as well as maximum field of view is too small to be suitable for *in vivo* use in humans. As such, all studies using micro-/nano-CT investigated *ex vivo* bone samples, which also influenced which joints were examined. Bone samples were usually obtained from joint replacement surgeries where articulating bone material was removed. The knee and hip joints are the most frequently replaced joints, hence those were the joints mainly investigated.

For *in vivo* measurement of microstructural parameters, it is recommended to use high resolution peripheral CT (HR-pQCT), not clinical CT or cone-beam CT. The resolution of current clinical CT technologies is not sufficient to image the microstructure of bone (200–400  $\mu\text{m}$ ). Only HR-pQCT has a spatial resolution high enough (58  $\mu\text{m}$ , 10 % MTF) to analyse bone microstructure *in vivo* (Supplementary Table 15) [25]. However, its limited field of view restricts its use to extremities (ankle, wrist, elbow, and small knees) which has somewhat limited the translation of microstructural measures from bench to bedside. A more recent development in CT technology, photon-counting CT may speed up the translatability of microstructural measures. Rather than detectors integrating the energy of a series of x-ray photons, photon-counting CT uses energy-resolving detectors in pulse mode, measuring individual packets of photon energy that exceed a given threshold. By virtue of the reduced pixel electrode size in a detector, this clinical CT with photon-counting detector is capable of imaging bone at a spatial resolution comparable to HR-pQCT, without being restricted to the extremities (Supplementary Table 15) [24,31,237–239]. Whilst it has been applied in few OA investigations, this has potential for direct translation of relevant microstructural parameters identified in microCT studies into clinical applications [240]. Furthermore, it reduces the limitation of bone sample availability. It allows for investigation of microstructural changes *in vivo* in any joint without relying on joint replacement surgeries to retrieve bone samples.

### 4.2. Bone adaptation – putting numbers to images

Bone adaptation parameters were largely used in OA pathogenesis investigations and methods validation studies. They are often used to confirm the presence of OA in images and to validate the reliability and

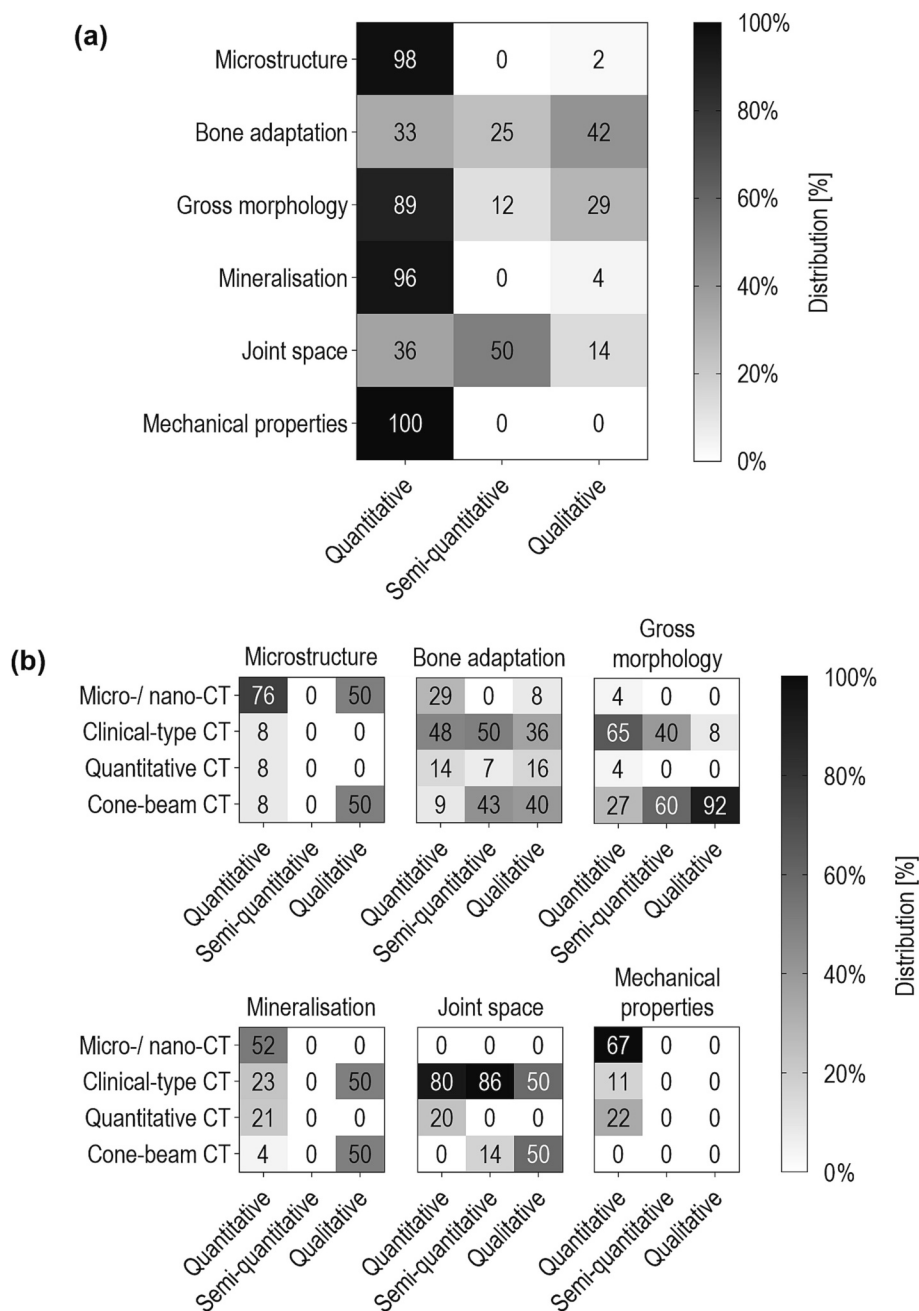


**Fig. 4.** Distribution of (a) quantitative, semi-quantitative and qualitative measures in each category (total of 100 % per category) and (b) CT technology used for measurement of all quantitative, semi-quantitative and qualitative parameters respectively in each category (total of 100 % per quantitative, semi-quantitative and qualitative group).

sensitivity of novel methods for OA detection. Bone adaptation was investigated at the TMJ more than any other joint. Imaging was mainly conducted with *in vivo* cone-beam CT, which is a standard CT technology used by dentists and maxillofacial specialists whose expertise includes TMJ disorders. Changes like bone erosion, osteophytes, and subchondral cysts were often seen as the basis of OA diagnosis at the TMJ using imaging [241,242], while in other locations loss of joint space (along with osteophyte formation) tended to carry more weight. Nevertheless, bone adaptation at a broad range of other joints was also analysed *ex vivo* using micro-/nano-CT and *in vivo* using clinical-type CT and quantitative CT. In clinical practice, the choice of CT technology for bone adaptation imaging should depend less on technological capability and more on the joint of interest. Cone-beam CT may be suitable for joints such as the TMJ and peripheral joints whereas clinical CT may be

more appropriate for hip, shoulder, and spinal joints. Features like bone cysts, osteophytes, sclerosis and bone erosion were frequently assessed qualitatively, only recording the presence of these features, or using semi-quantitative scoring. They seem to be reliable features for OA diagnosis and if the presence or absence of bone adaptation was merely used to diagnose OA, this may suffice. However, it raises the question of how disease progression and treatment efficacy might be assessed using these properties. The judgement of the person scoring the images introduces a subjective component with inter- and intra-observer errors [243]. One's image interpretations may vary from one time point to the next, particularly in unclear cases and different people may interpret the same image differently. Additionally, score differences have been observed between grading systems [243]. Quantifying the observed phenomena by measuring size, area and volume as suggested by

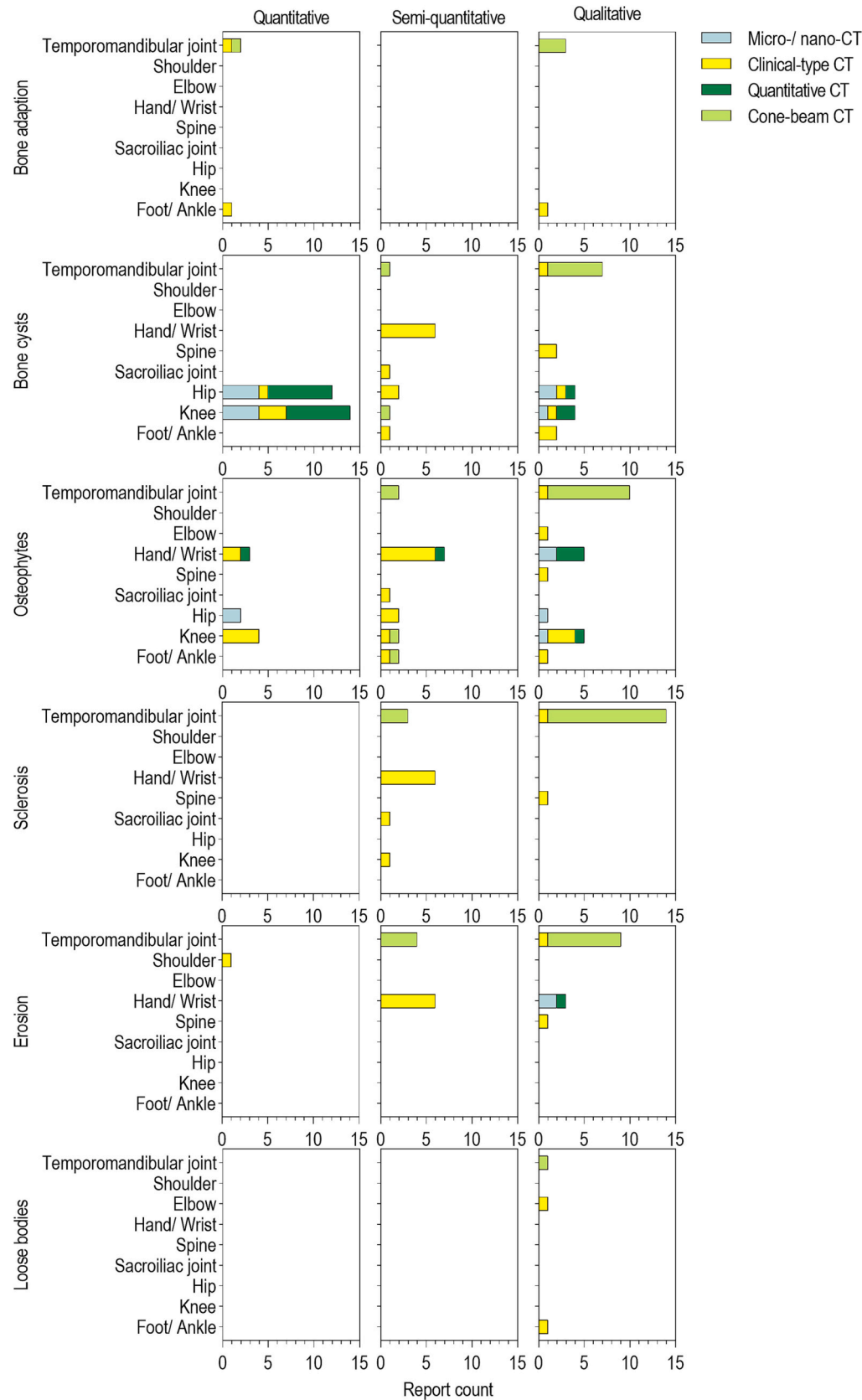


**Fig. 5.** Report count of quantitative, semi-quantitative and qualitative bone adaption parameters, anatomical location and CT group with which they were measured. One quantitative parameter (void fraction, measured in shoulder with clinical-type CT) is not included in figure.



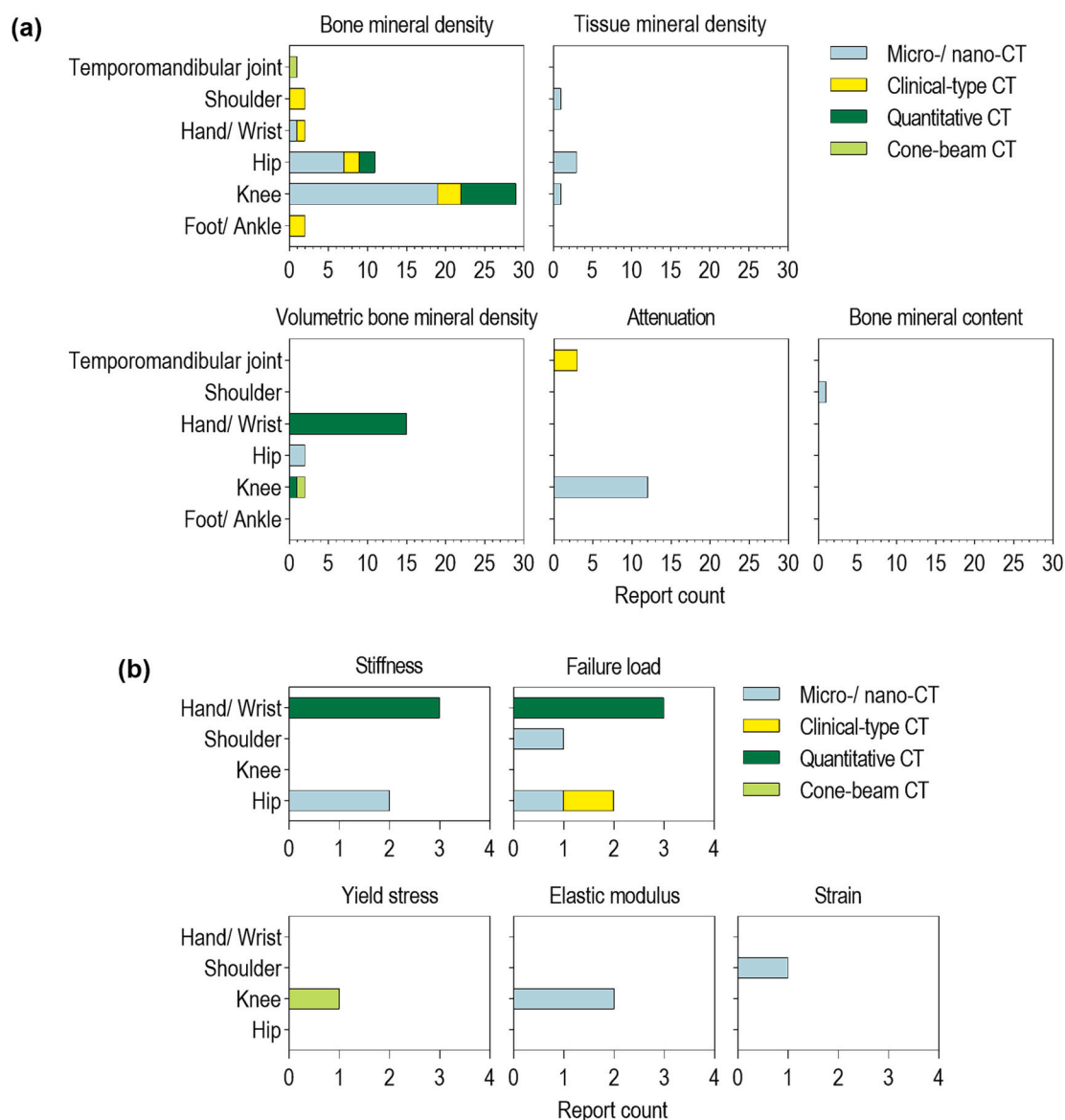


**Fig. 6.** Report count of quantitative parameters measuring (a) mineralisation, anatomical location analysed and CT group used for measurement (three qualitative parameters (Attenuation (2×): knee, clinical-type CT; Free calcifications: TMJ, cone-beam CT) are not included in the figure) and (b) mechanical properties, anatomical location analysed and CT group used for measurement.

multiple studies could aid with this [31,48,65,120,121,127,133,138,139,142,143,181,183–185,197,216,222,229,231], particularly with the knowledge of the role that bone plays in OA, potentially allowing a more accurate evaluation of disease progression and treatment efficacy.

#### 4.3. Gross morphology – the wild west of descriptions

Gross morphology was of particular interest in pathogenesis studies investigating OA progression and connections between alignment, joint morphology, and OA development. It was also analysed to characterise different disease phenotypes. Most parameters describing the morphology of osteoarthritic bone evaluate alignment angles and changes to bone shape in images obtained *in vivo* with clinical-type CT. In order to measure such features, the chosen CT technology does not need to produce images of the highest resolution but the field of view of the scanner needs to be large enough to image the whole joint. Hence, cone-beam CT may suffice for smaller joints like the TMJ and ankle joints whereas clinical CT is required for larger joints like the knee, hip, or shoulder joints. In the shoulder, alignment measurements such as

glenoid version and inclination are frequently reported in relation to osteoarthritis, but reference lines and anatomical references used for measurements varied between methods [35,40,54,135,136]. Likewise, subluxation of the metacarpal bone in the hand was reported as a measurement that captures osteoarthritic changes but approaches and anatomical references differed between reports [50,132]. Multiple approaches for capturing bone shape changes were recorded. Cevdanes et al. [195] and Lynch et al. [171] employed statistical shape modelling to investigate changes to the bone in the TMJs and knee joint respectively. Knowles et al. [143] attempted to analyse bone loss in the glenoid of Walch classification B2 shoulders by defining a line of erosion which separates the glenoid into paleoglenoid and neoglenoid in images obtained from clinical-type CT. They found the position and angle of this line of erosion shifted with severity of OA, indicating asymmetric bone loss. Taken together, these studies suggest angles are easily measured for a trained individual and could be helpful in diagnosing OA and evaluating disease risk and progression. Such morphological changes seem likely to offer valuable insight into a pre-determined risk for OA and evaluation of disease progression once manifested. However, there

seems to be little consensus on measurement methods and approaches. If key measurements and standardised methods could be identified, they may not only serve as morphological descriptions but also add value to indirectly quantifying bone adaptation.

#### 4.4. Mineralisation – variability in the face of reliability

Bone mineral density is commonly used to assess bone quality in diseases such as osteoporosis [244–246], yet OA is known to also cause substantial changes in bone mineralisation [247,248]. Studies investigating bone mineralisation changes in OA predominantly involved quantitative measurements in knee and hip joints using *ex vivo* micro-CT and nano-CT, although *in vivo* analysis with quantitative and clinical-type CT also contributed 20 % each. The recommended CT technologies to measure mineralisation of bone are micro-/nano-CT for *ex vivo* and quantitative CT for *in vivo* measurements. The scanning of hydroxyapatite phantoms allows for quantitative assessment of mineralisation. Mainly studies investigating pathogenesis and disease phenotypes used mineralisation parameters. They often focus on the role of bone mineralisation in OA or phenotypical differences in mineralisation. Whilst most studies concluded that OA influenced bone mineralisation, the precise effect of OA on mineralisation remains unclear. Abnormal bone remodelling leads to osteophytes, cysts and sclerosis, which can make mineralisation greatly location- and depth-dependent. Johnston et al. [225], Sannmann et al. [227], and Myller et al. [203] showed how different locations in the knee have different mineral contents. They found mineralisation in superficial layers to be highest, decreasing with increasing bone depth. Furthermore, meniscal coverage was found to result in decreased mineral content in the underlying bone. Similarly, Knowles et al. [142] and Letissier et al. [47] showed that the shape and wear pattern in shoulder joints influenced bone mineralisation. Furthermore, the development of cysts and osteophytes were shown to affect mineral content. Measurements varied depending on whether the void caused by cysts was considered in global analysis or how close to the cysts local measurements were taken [65,230]. Additionally, the type of mineralisation measure chosen for the analysis may affect any conclusions made. Bone mineral density is a mineralisation measure of a mixed bone volume containing both trabecular and cortical bone whereas tissue mineral density measures the mineral density within cortical bone, hence results may vary between them. As it currently stands, mineralisation does not seem to be a powerful measure for OA. Global metrics are often biased and fail to do justice to the local differences due to the heterogeneity of mineral distribution in OA derived from local disease features. Clear definitions and standards regarding measurement location are necessary to improve the reliability of mineralisation parameters. If this is achieved, they could become valuable parameters that are easy to obtain and clinically relevant.

#### 4.5. Joint space – a ghost measure of subchondral bone

Radiography is the most widely used clinical radiological method used to assess OA. However, it cannot accurately image soft tissue and is unable to depict cartilage directly, hence the need to use MRI (and to some extent ultrasound) for the assessment of cartilage and other joint soft tissue structures. Consequently, joint space narrowing has been used as a measurement that encompasses both cartilage health and meniscal damage at the knee. In the context of subchondral bone, it has been of particular interest in combination with bone adaptation parameters to confirm OA in images. Additionally, it was of interest in studies validating novel methods to measure joint space, making use of the advantages CT holds. The translation to CT has mainly occurred in clinical-type CT for the *in vivo* assessment of various joints across many anatomical locations except for one study that analysed vacuum phenomena *ex vivo* at sacroiliac joints. The important factor for CT technology choice here is also field of view and the joint of interest. Larger joints will require clinical-type CT whereas smaller joints may be imaged

with cone-beam CT. Half of the included studies evaluated joint space semi-quantitatively, however, studies by Segal et al. [211,249,250] and Turmezei et al. [251–253] show that CT provides a more precise quantitative measure of joint space compared to radiography due to it being 3-D, thus increasing its sensitivity in the assessment of OA. Therefore, in the context of OA research, more precise and quantitative information related to joint space loss, assumed to be from factors such as cartilage degeneration and meniscal extrusion, captured by high resolution images of bone could be beneficial. Alternatively, CT arthrography has been shown to be an accurate method to assess cartilage directly using CT in combination with an intra-articular contrast agent [254–256].

#### 4.6. Mechanical properties – estimating tissue quality

Mechanical properties of bone can be estimated with finite element (FE) modelling based on images obtained with CT. To create an FE model, voxels from the CT image are converted to elements, which are then assigned material properties (elastic modulus and Poisson ratio). Using this model, loading simulations can be performed to analyse and estimate mechanical properties of interest. Similarly, discrete element (DE) analysis is a computational method to estimate intra-articular contact stress. It is a faster method to obtain comparable information to FE analysis, but it sacrifices material property definitions and continuum mechanics, which takes deformation and transmission of force into account. Neither of these computational methods are commonly used to assess subchondral bone in OA because they are usually conducted on whole bones rather than bone compartments such as subchondral bone. In the few studies captured here, micro-/nano-CT and quantitative CT were mostly used for *ex vivo* FE analysis of knee, hand/wrist and hip joints. Crucial factors for FE analysis are bone shape and microstructure as well as mineralisation. Therefore, micro-/nano-CT and HR-pQCT are the recommended CT types to image joints for FE analysis. The studies that investigated mechanical properties of bone focused on the pathogenesis of OA. They investigated the impact of OA on parameters like stiffness, failure load and elastic modulus. FE and DE analysis permit different loading scenarios to be explored to aid in the assessment of OA progression and therapeutic efficacy. Accordingly, FE and DE analysis could be considered for subchondral bone assessment in OA.

#### 4.7. Limitations

It is important to note that for joint space and mechanical properties, the search strategy did not capture the full field. The search parameters and inclusion criteria were aimed at subchondral bone, therefore many studies investigating joint space with CT in OA were not included because they did not mention subchondral bone. Furthermore, limited studies investigating mechanical properties were picked up by the search strategy due to them using FE modelling for whole bone analysis rather than recognising subchondral bone as a separate entity. Nevertheless, the available literature found via this search strategy highlights that they are relevant to the field of OA imaging with CT.

Finally, the large scope of this review enabled a broad overview of CT parameters used for the assessment of subchondral bone in OA. Subsequent reviews and scientific studies could focus on single parameter categories to deepen the discussion around specific parameters and their usefulness in different applications as well as appropriate CT technologies for their analysis.

## 5. Conclusion

With CT gaining popularity in OA research, this review has provided important insight into current applications for the assessment of OA. Six main categories of microstructure, bone adaptation, gross morphology, mineralisation, joint space and mechanical properties, were identified as

being of interest in OA analysis with CT. This review can serve as a resource to anyone looking to use CT as an imaging modality to analyse bone in OA via a multitude of approaches. We have highlighted clinically meaningful parameter categories as well as categories that have potential to be translated into clinical application. Finally, we have stressed the importance of quantification of parameters to improve sensitivity and reproducibility, and the need for consistency and standardisation of protocols necessary for parameters in order to add value to future OA research and clinical practice.

## Funding source

This research did not receive any specific grant from funding agencies in the public, commercial, or not-for-profit sectors.

## CRediT authorship contribution statement

**Jemima E. Shadow:** Writing – review & editing, Writing – original draft, Validation, Methodology, Investigation, Formal analysis, Data curation. **David Maxey:** Investigation, Data curation. **Toby O. Smith:** Writing – review & editing, Visualization, Supervision, Methodology, Investigation. **Mikko A.J. Finnilä:** Writing – review & editing, Validation, Conceptualization. **Sarah L. Manske:** Writing – review & editing, Validation, Conceptualization. **Neil A. Segal:** Writing – review & editing, Validation, Conceptualization. **Andy Kin On Wong:** Writing – review & editing, Validation, Conceptualization. **Rachel A. Davey:** Writing – review & editing, Validation, Supervision. **Tom Turmezei:** Writing – review & editing, Visualization, Validation, Supervision, Formal analysis, Conceptualization. **Kathryn S. Stok:** Writing – review & editing, Visualization, Validation, Supervision, Project administration, Methodology, Investigation, Formal analysis, Conceptualization.

## Declaration of competing interest

The authors declare no conflict of interest.

## Data availability

Data will be made available on request.

## Appendix A. Supplementary data

Supplementary data to this article can be found online at <https://doi.org/10.1016/j.bone.2023.116948>.

## References

- [1] R. Altman, et al., Development of criteria for the classification and reporting of osteoarthritis: classification of osteoarthritis of the knee, *Arthritis Rheum.* 29 (8) (1986) 1039–1049.
- [2] D.K. Dedrick, et al., A longitudinal study of subchondral plate and trabecular bone in cruciate-deficient dogs with osteoarthritis followed up for 54 months, *Arthritis Rheum.* 36 (10) (1993) 1460–1467.
- [3] D.T. Felson, et al., Bone marrow edema and its relation to progression of knee osteoarthritis, *Ann. Intern. Med.* 139 (5 Part 1) (2003) 330–336.
- [4] T. Muraoka, et al., Role of subchondral bone in osteoarthritis development: a comparative study of two strains of Guinea pigs with and without spontaneously occurring osteoarthritis, *Arthritis Rheum.* 56 (10) (2007) 3366–3374.
- [5] S.R. Goldring, Alterations in periarticular bone and cross talk between subchondral bone and articular cartilage in osteoarthritis, *Ther. Adv. Musculoskelet. Dis.* 4 (4) (2012) 249–258.
- [6] S.R. Goldring, M.B. Goldring, Changes in the osteochondral unit during osteoarthritis: structure, function and cartilage–bone crosstalk, *Nat. Rev. Rheumatol.* 12 (11) (2016) 632–644.
- [7] M. Samim, et al., 3D-MRI versus 3D-CT in the evaluation of osseous anatomy in femoroacetabular impingement using Dixon 3D FLASH sequence, *Skelet. Radiol.* 48 (3) (2019) 429–436.
- [8] L. Stillwater, et al., 3D-MR vs. 3D-CT of the shoulder in patients with glenohumeral instability, *Skelet. Radiol.* 46 (3) (2017) 325–331.
- [9] M.L. Bouxsein, et al., Guidelines for assessment of bone microstructure in rodents using micro-computed tomography, *J. Bone Miner. Res.* 25 (7) (2010) 1468–1486.
- [10] M.K. Kalra, et al., Multidetector computed tomography technology: current status and emerging developments, *J. Comput. Assist. Tomogr.* 28 (2004) S2–S6.
- [11] I. Nasseh, W. Al-Rawi, Cone beam computed tomography, *Dent. Clinics* 62 (3) (2018) 361–391.
- [12] R. Burkart, et al., Magnetic resonance imaging–based assessment of cartilage loss in severe osteoarthritis: accuracy, precision, and diagnostic value, *Arthritis Rheum.* 44 (9) (2001) 2072–2077.
- [13] F. Eckstein, et al., Magnetic resonance imaging (MRI) of articular cartilage in knee osteoarthritis (OA): morphological assessment, *Osteoarthritis. Cartil.* 14 (2006) 46–75.
- [14] P. Conaghan, et al., MRI and non-cartilaginous structures in knee osteoarthritis, *Osteoarthritis. Cartil.* 14 (2006) 87–94.
- [15] F.W. Roemer, et al., Imaging in osteoarthritis, *Osteoarthritis. Cartil.* 30 (7) (2022) 913–934.
- [16] D.T. Felson, et al., A new approach yields high rates of radiographic progression in knee osteoarthritis, *J. Rheumatol.* 35 (10) (2008) 2047–2054.
- [17] M. Kinds, et al., Influence of variation in semiflexed knee positioning during image acquisition on separate quantitative radiographic parameters of osteoarthritis, measured by knee images digital analysis, *Osteoarthritis. Cartil.* 20 (9) (2012) 997–1003.
- [18] P. Durongbhan, et al., Quantitative morphometric analysis in tibiofemoral joint osteoarthritis imaging: a literature review, *Osteoarthritis. Imaging.* 2 (2023), 100088.
- [19] L. Menashe, et al., The diagnostic performance of MRI in osteoarthritis: a systematic review and meta-analysis, *Osteoarthritis. Cartil.* 20 (1) (2012) 13–21.
- [20] N.V. Koninklijke Philips, Access CT: Redefining Value in CT, Philips, 2014 January 2014 cited 28 September 2023, <https://www.philips.com.au/healthcare/product/HCTN480/access-ct-redefining-value-in-ct#documents>.
- [21] Siemens Healthcare GmbH, SOMATOM Force: Get Two Steps Ahead With Dual Source CT, Siemens Healthineers, 2023 [cited 28 September 2023], <https://www.siemens-healthineers.com/en-au/computed-tomography/dual-source-ct/somatom-force>.
- [22] GE Healthcare, Manuals & Documents. GE Healthcare, cited 28 September 2023, <https://www.gehealthcare.com/support/manuals>, 2023.
- [23] R. Kijowski, J. Fritz, Emerging technology in musculoskeletal MRI and CT, *Radiology* 306 (1) (2023) 6–19.
- [24] Siemens Healthcare Pty Ltd, NAEOTOM Alpha With Quantum Technology: CT Redefined, Siemens Healthineers, 2023 [cited 28 September 2023], <https://www.siemens-healthineers.com/en-au/computed-tomography/photon-counting-ct-scanner/naeotom-alpha>.
- [25] SCANCO Medical AG, XtremeCT II. SCANCO Medical, cited 28 September 2023, <https://www.scanco.ch/xtremectii.html>, 2023.
- [26] T. Oláh, M. Cucchiari, H. Madry, Subchondral bone remodeling patterns in larger animal models of meniscal injuries inducing knee osteoarthritis—a systematic review, *Knee Surg. Sports Traumatol. Arthrosc.* (2023) 1–19.
- [27] T. Fukuda, et al., CT in osteoarthritis: its clinical role and recent advances, *Skelet. Radiol.* (2022) 1–12.
- [28] M.J. Page, et al., The PRISMA 2020 statement: an updated guideline for reporting systematic reviews, *Inter. J. Surg.* 88 (2021), 105906, <https://doi.org/10.1016/j.ijsu.2021.105906>.
- [29] J. Akers, R. Aguiar-Ibáñez, A. Baba-Akbari, Systematic Reviews: CRD's Guidance for Undertaking Reviews in Health Care, Centre for Reviews and Dissemination, University of York, 2009. [https://www.york.ac.uk/media/crd/Systematic\\_Reviews.pdf](https://www.york.ac.uk/media/crd/Systematic_Reviews.pdf).
- [30] G.A. Wells, et al., The Newcastle-Ottawa Scale (NOS) for Assessing the Quality of Nonrandomised Studies in Meta-analyses, 2000. Oxford.
- [31] C. Chappard, et al., Virtual monoenergetic images from photon-counting spectral computed tomography to assess knee osteoarthritis, *Eur. Radiol. Exp.* 6 (1) (2022) 10.
- [32] W.P. Gielis, et al., Osteoarthritis in pseudoxanthoma elasticum patients: an explorative imaging study, *J. Clin. Med.* 9 (12) (2020) 1–10.
- [33] S.S. Karhula, et al., Quantifying subresolution 3D morphology of bone with clinical computed tomography, *Ann. Biomed. Eng.* 48 (2) (2020) 595–605.
- [34] T. Oláh, et al., Quantifying the human subchondral trabecular bone microstructure in osteoarthritis with clinical CT, *Adv. Sci. (Weinheim, Ger.)* 9 (23) (2022), e2201692.
- [35] A.W. Aleem, et al., Association between rotator cuff muscle size and glenoid deformity in primary glenohumeral osteoarthritis, *J. Bone Joint Surg. (Am. Vol.)* 101 (21) (2019) 1912–1920.
- [36] S. Beeler, et al., Acromial roof in patients with concentric osteoarthritis and massive rotator cuff tears: multiplanar analysis of 115 computed tomography scans, *J. Shoulder Elb. Surg.* 27 (10) (2018) 1866–1876.
- [37] S. Beeler, et al., Different acromial roof morphology in concentric and eccentric osteoarthritis of the shoulder: a multiplane reconstruction analysis of 105 shoulder computed tomography scans, *J. Shoulder Elb. Surg.* 27 (12) (2018) e357–e366.
- [38] S. Beeler, et al., Critical shoulder angle: acromial coverage is more relevant than glenoid inclination, *J. Orthop. Res.* 37 (1) (2019) 205–210.
- [39] D.J. Bokor, et al., Does the osteoarthritic shoulder have altered rotator cuff vectors with increasing glenoid deformity? An in silico analysis, *J. Shoulder Elb. Surg.* 31 (12) (2022) e575–e585.
- [40] K. Chan, et al., Characterization of the Walch B3 glenoid in primary osteoarthritis, *J. Shoulder Elb. Surg.* 26 (5) (2017) 909–914.
- [41] J.S. Chang, et al., Why do subchondral cysts occur at the medial aspect of the femoral head in hip dysplasia?, in: *HIP International*, 2020.

- [42] Y. Dai, et al., Association of patellofemoral morphology and alignment with the radiographic severity of patellofemoral osteoarthritis, *J. Orthop. Surg. Res.* 16 (1) (2021) 548.
- [43] K.W. Donohue, et al., The association between rotator cuff muscle fatty infiltration and glenoid morphology in glenohumeral osteoarthritis, *J. Bone Joint Surg. Am.* 100 (5) (2018) 381–387.
- [44] M.-O. Gaudi, et al., Identification of threshold pathoanatomic metrics in primary glenohumeral osteoarthritis, *J. Shoulder Elb. Surg.* 30 (10) (2021) 2270–2282.
- [45] R.K. Gebre, et al., Detecting hip osteoarthritis on clinical CT: a deep learning application based on 2-D summation images derived from CT, *Osteoporos. Int.* 33 (2) (2022) 355–365.
- [46] T.B. Hansen, et al., Computed tomography improves intra-observer reliability, but not the inter-observer reliability of the Eaton-Glickel classification, *J. Hand Surg. Eur. Vol.* 38 (2) (2013) 187–191.
- [47] H. Letissier, et al., Glenoid subchondral bone density in osteoarthritis: a comparative study of asymmetric and symmetric erosion patterns, *Orthop. Traumatol. Surg. Res.* 106 (6) (2020) 1127–1134.
- [48] S.C. Mastbergen, et al., Subchondral bone changes after joint distraction treatment for end stage knee osteoarthritis, *Osteoarthr. Cartil.* 30 (7) (2022) 965–972.
- [49] M.S. Park, et al., Facet joint degeneration of the cervical spine: a computed tomographic analysis of 320 patients, *Spine* 39 (12) (2014) E713–E718.
- [50] M.S. Saltzherr, et al., Computed tomography for the detection of thumb base osteoarthritis: comparison with digital radiography, *Skelet. Radiol.* 42 (5) (2013) 715–721.
- [51] J. Schmalzl, et al., Proximal humeral fracture morphology in patients with advanced osteoarthritis: an observational study in a surgically treated cohort, *J. Orthop. Surg.* 28 (3) (2020).
- [52] D.R. Shukla, et al., Intraobserver and interobserver reliability of the modified Walch classification using radiographs and computed tomography, *J. Shoulder Elb. Surg.* 28 (4) (2019) 625–630.
- [53] A. Siddiqi, et al., Osseous morphological differences in knee osteoarthritis, *J. Bone Joint Surg. Am.* 104 (9) (2022) 805–812.
- [54] M.J. Siebert, et al., Qualitative and quantitative analysis of glenoid bone stock and glenoid version: inter-reader analysis and correlation with rotator cuff tendinopathy and atrophy in patients with shoulder osteoarthritis, *Skelet. Radiol.* 49 (6) (2020) 985–993.
- [55] F. Verhaegen, et al., Quantitative statistical shape model-based analysis of humeral head migration, part 2: shoulder osteoarthritis, *J. Orthop. Res.* 41 (1) (2023) 21–31.
- [56] K.E. Walker, et al., Progression of glenoid morphology in glenohumeral osteoarthritis, *J. Bone Joint Surg. Am.* 100 (1) (2018) 49–56.
- [57] S.A. Badve, et al., Occipito-atlanto-axial osteoarthritis: a cross sectional clinico-radiological prevalence study in high risk and general population, *Spine* 35 (4) (2010) 434–438.
- [58] R. Husic, et al., Ultrasound in osteoarthritis of the hand: a comparison to computed tomography and histology, *Rheumatology (Oxford, England)* 61 (SI) (2022) SI73–SI80.
- [59] C. Ma, et al., Association between radiographic hand osteoarthritis and bone microarchitecture in a population-based sample, *Arthritis Res. Ther.* 24 (1) (2022) 223.
- [60] K. Martini, et al., Value of tomosynthesis for lesion evaluation of small joints in osteoarthritic hands using the OARS score, *Osteoarthr. Cartil.* 24 (7) (2016) 1167–1171.
- [61] D. Simon, et al., Bone mass, bone microstructure and biomechanics in patients with hand osteoarthritis, *J. Bone Miner. Res. Off. J. Am. Soc. Bone Miner. Res.* 35 (9) (2020) 1695–1702.
- [62] S. Touraine, et al., Chondrocalcinosis of femoro-tibial and proximal Tibio-fibular joints in cadaveric specimens: a high-resolution CT imaging study of the calcification distribution, *PLoS One* 8 (1) (2013), e54955.
- [63] Y. Chen, et al., Subchondral trabecular rod loss and plate thickening in the development of osteoarthritis, *J. Bone Miner. Res.* 33 (2) (2018) 316–327.
- [64] Y. Chen, et al., Attenuation of subchondral bone abnormal changes in osteoarthritis by inhibition of SDF-1 signaling, *Osteoarthr. Cartil.* 25 (6) (2017) 986–994.
- [65] Y. Chen, et al., Bone turnover and articular cartilage differences localized to subchondral cysts in knees with advanced osteoarthritis, *Osteoarthr. Cartil.* 23 (12) (2015) 2174–2183.
- [66] Z. Chen, et al., Inhibition of Nrf2/HO-1 signaling leads to increased activation of the NLRP3 inflammasome in osteoarthritis, *Arthritis Res. Ther.* 21 (1) (2019) 300.
- [67] L. Chu, et al., Articular cartilage degradation and aberrant subchondral bone remodeling in patients with osteoarthritis and osteoporosis, *J. Bone Miner. Res.* 35 (3) (2020) 505–515.
- [68] L. Chu, et al., Different subchondral trabecular bone microstructure and biomechanical properties between developmental dysplasia of the hip and primary osteoarthritis, *J. Orthop. Translat.* 22 (2020) 50–57.
- [69] M. Dabrowski, et al., Subchondral bone relative area and density in human osteoarthritic femoral heads assessed with micro-ct before and after mechanical embedding of the innovative multi-spiked connecting scaffold for resurfacing the endoprostheses: a pilot study, *J. Clin. Med.* 10 (13) (2021) 2937.
- [70] M. Ding, S. Overgaard, 3-D microarchitectural properties and rod- and plate-like trabecular morphometric properties of femur head cancellous bones in patients with rheumatoid arthritis, osteoarthritis, and osteoporosis, *J. Orthop. Translat.* 28 (2021) 159–168.
- [71] M. Ding, S. Overgaard, Degenerations in global morphometry of cancellous bone in rheumatoid arthritis, osteoarthritis and osteoporosis of femoral heads are similar but more severe than in ageing controls, *Calcif. Tissue Int.* 110 (1) (2022) 57–64, <https://doi.org/10.1007/s00223-021-00889-2>.
- [72] K. Endo, et al., Magnetic resonance imaging T1 and T2 mapping provide complementary information on the bone mineral density regarding cancellous bone strength in the femoral head of postmenopausal women with osteoarthritis, *Clin. Biomech.* 65 (2019) 13–18.
- [73] M.A.J. Finnila, et al., Association between subchondral bone structure and osteoarthritis histopathological grade, *J. Orthop. Res.* 35 (4) (2017) 785–792.
- [74] B. Gatenholm, et al., Spatially matching morphometric assessment of cartilage and subchondral bone in osteoarthritic human knee joint with micro-computed tomography, *Bone* 120 (asr, 8504048) (2019) 393–402.
- [75] S. Haberkamp, et al., Analysis of spatial osteochondral heterogeneity in advanced knee osteoarthritis exposes influence of joint alignment, *Sci. Transl. Med.* 12 (562) (2020) no pagination.
- [76] I. Hadjab, et al., Electromechanical properties of human osteoarthritic and asymptomatic articular cartilage are sensitive and early detectors of degeneration, *Osteoarthr. Cartil.* 26 (3) (2018) 405–413.
- [77] X. Han, et al., Association between knee alignment, osteoarthritis disease severity, and subchondral trabecular bone microarchitecture in patients with knee osteoarthritis: a cross-sectional study, *Arthritis Res. Ther.* 22 (1) (2020) 203.
- [78] Y. Huang, et al., 3D high-frequency ultrasound imaging of cartilage-bone interface compared with micro-CT, *Biomed. Res. Int.* 2020 (2020) 6906148.
- [79] Y.P. Huang, et al., High-frequency ultrasound imaging of tidemark in vitro in advanced knee osteoarthritis, *Ultrasound Med. Biol.* 44 (1) (2018) 94–101.
- [80] A. Jaiprakash, et al., Phenotypic characterization of osteoarthritic osteocytes from the sclerotic zones: a possible pathological role in subchondral bone sclerosis, *Int. J. Biol. Sci.* 8 (3) (2012) 406–417.
- [81] W.G. Jones, et al., Multipotential stromal cells in the talus and distal tibia in ankle osteoarthritis - presence, potency and relationships to subchondral bone changes, *J. Cell. Mol. Med.* 25 (1) (2021) 259–271.
- [82] K.K. Kim, Regional distribution of stress on the distal femur in advanced osteoarthritis, *J. Bone Metab.* 25 (3) (2018) 175–180.
- [83] W. Kiyan, et al., Ultrasound parameters for human osteoarthritic subchondral bone ex vivo: comparison with micro-computed tomography parameters, *Ultrasound Med. Biol.* 44 (10) (2018) 2115–2130.
- [84] K. Kizaki, et al., Microstructure of osteophytes in medial knee osteoarthritis, *Clin. Rheumatol.* 37 (10) (2018) 2893–2896.
- [85] A. Lahm, et al., Varying development of femoral and tibial subchondral bone tissue and their interaction with articular cartilage during progressing osteoarthritis, *Arch. Orthop. Trauma Surg.* 140 (12) (2020) 1919–1930.
- [86] A. Lahm, et al., Correlation between 3D microstructural and 2D histomorphometric properties of subchondral bone with healthy and degenerative cartilage of the knee joint, *Histol. Histopathol.* 29 (11) (2014) 1477–1488.
- [87] B.A. Lakin, et al., Contrast-enhanced CT facilitates rapid, non-destructive assessment of cartilage and bone properties of the human metacarpal, *Osteoarthr. Cartil.* 23 (12) (2015) 2158–2166.
- [88] A.T. Lee, et al., Trapezium trabecular morphology in carpometacarpal arthritis, *J. Hand. Surg. [Am.]* 38 (2) (2013) 309–315.
- [89] G. Li, et al., Identical subchondral bone microarchitecture pattern with increased bone resorption in rheumatoid arthritis as compared to osteoarthritis, *Osteoarthr. Cartil.* 22 (12) (2014) 2083–2092.
- [90] G. Li, et al., Influence of age and gender on microarchitecture and bone remodeling in subchondral bone of the osteoarthritic femoral head, *Bone* 77 (asr, 8504048) (2015) 91–97.
- [91] Y. Li, et al., Subchondral bone microarchitecture and mineral density in human osteoarthritis and osteoporosis: a regional and compartmental analysis, *J. Orthop. Res.* 39 (12) (2021) 2568–2580.
- [92] Z.-C. Li, et al., Difference in subchondral cancellous bone between postmenopausal women with hip osteoarthritis and osteoporotic fracture: implication for fatigue microdamage, bone microarchitecture, and biomechanical properties, *Arthritis Rheum.* 64 (12) (2012) 3955–3962.
- [93] A.B. Lovati, et al., A comparative study of diagnostic and imaging techniques for osteoarthritis of the trapezium, *Rheumatology* 54 (1) (2015) 96–103.
- [94] L.-S. Lu, et al., Genome-wide expression profiles of subchondral bone in osteoarthritis, *Arthritis Res. Ther.* 15 (6) (2013) R190.
- [95] G. Mitton, et al., A degenerative medial meniscus retains some protective effect against osteoarthritis-induced subchondral bone changes, *Bone Rep.* 12 (2020) no pagination.
- [96] M.J. Montoya, et al., Microstructural trabecular bone from patients with osteoporotic hip fracture or osteoarthritis: its relationship with bone mineral density and bone remodelling markers, *Maturitas* 79 (3) (2014) 299–305.
- [97] D. Muratovic, et al., Bone marrow lesions in knee osteoarthritis: regional differences in tibial subchondral bone microstructure and their association with cartilage degeneration, *Osteoarthr. Cartil.* 27 (11) (2019) 1653–1662.
- [98] C. Netzer, et al., Comparative analysis of bone structural parameters reveals subchondral cortical plate resorption and increased trabecular bone remodeling in human facet joint osteoarthritis, *Int. J. Mol. Sci.* 19 (3) (2018) 14.
- [99] H. Nieminen, et al., 3D histopathological grading of osteochondral tissue using contrast-enhanced micro-computed tomography, *Osteoarthr. Cartil.* 25 (10) (2017) 1680–1689.
- [100] D.Y. Park, et al., Subchondral bone scan uptake correlates with articular cartilage degeneration in osteoarthritic knees, *Int. J. Rheum. Dis.* 20 (10) (2017) 1393–1402.



- [101] A.M. Philp, et al., Resistin promotes the abnormal type I collagen phenotype of subchondral bone in obese patients with end stage hip osteoarthritis, *Sci. Rep.* 7 (1) (2017) 4042.
- [102] B. Pouran, et al., Solute transport at the interface of cartilage and subchondral bone plate: effect of micro-architecture, *J. Biomech.* 52 (0157375, hif) (2017) 148–154.
- [103] P. Pu, et al., Protein-Degrading Enzymes in Osteoarthritis, *Proteol. Enzyme Osteoarthr.* 159 (1) (2021) 54–66.
- [104] S. Rapagna, et al., Tibial cartilage, subchondral bone plate and trabecular bone microarchitecture in varus- and valgus-osteoarthritis versus controls, *J. Orthop. Res.* 39 (9) (2021) 1988–1999.
- [105] N. Reina, et al., BMI-related microstructural changes in the tibial subchondral trabecular bone of patients with knee osteoarthritis, *J. Orthop. Res.* 35 (8) (2017) 1653–1660.
- [106] B.C. Roberts, et al., Joint loading and proximal tibia subchondral trabecular bone microarchitecture differ with walking gait patterns in end-stage knee osteoarthritis, *Osteoarthr. Cartil.* 25 (10) (2017) 1623–1632.
- [107] B.C. Roberts, et al., Relationships between in vivo dynamic knee joint loading, static alignment and tibial subchondral bone microarchitecture in end-stage knee osteoarthritis, *Osteoarthr. Cartil.* 26 (4) (2018) 547–556.
- [108] B.C. Roberts, et al., Systematic mapping of the subchondral bone 3D microarchitecture in the human tibial plateau: variations with joint alignment, *J. Orthop. Res.* 35 (9) (2017) 1927–1941.
- [109] M. Ryan, et al., A new approach to comprehensively evaluate the morphological properties of the human femoral head: example of application to osteoarthritic joint, *Sci. Rep.* 10 (1) (2020) 5538.
- [110] M.J. Steinbeck, et al., Identifying patient-specific pathology in osteoarthritis development based on MicroCT analysis of subchondral trabecular bone, *J. Arthroplast.* 31 (1) (2016) 269–277.
- [111] I. Tamimi, et al., Composition and characteristics of trabecular bone in osteoporosis and osteoarthritis, *Bone* 140 (2020) 115558 (Tamimi, Sanchez-Siles, Gonzalez-Quevedo, Garcia, Garcia-de-Quevedo) Department of Orthopedic Surgery, Regional University Hospital of Malaga, Spain.
- [112] S. Tassani, et al., Dependence of trabecular structure on bone quantity: a comparison between osteoarthritic and non-pathological bone, *Clin. Biomech.* 26 (6) (2011) 632–639.
- [113] A. Tsoukidas, et al., The effect of osteoarthritis on the regional anatomical variation of subchondral trabecular bone in the femoral head, *Clin. Biomech. (Bristol, Avon)* 30 (5) (2015) 418–423.
- [114] Q. Wei, et al., Abnormal subchondral bone remodeling and its association with articular cartilage degradation in knees of type 2 diabetes patients, *Bone Res.* 5 (2017) 17034 (Chen, Wei, Zhao) Department of Bone and Joint Surgery, First Affiliated Hospital, Guangxi Medical University, China.
- [115] C.Y. Wen, et al., Bone loss at subchondral plate in knee osteoarthritis patients with hypertension and type 2 diabetes mellitus, *Osteoarthr. Cartil.* 21 (11) (2013) 1716–1723.
- [116] D. Wu, et al., Association of microstructural and mechanical properties of cancellous bone and their fracture risk assessment tool scores, *Int. J. Clin. Exp. Med.* 8 (3) (2015) 3956–3964.
- [117] J. Xiao, et al., Correlation between neuropeptide distribution, cancellous bone microstructure and joint pain in postmenopausal women with osteoarthritis and osteoporosis, *Neuropeptides* 56 (2016) 97–104.
- [118] C. Zhang, et al., Subchondral bone deterioration in femoral heads in patients with osteoarthritis secondary to hip dysplasia: a case-control study, *J. Orthop. Translat.* 24 (2020) 190–197 (Li, Zhang) Department of Orthopaedic Surgery, Shanghai Jiao Tong University Affiliated Sixth People's Hospital, Shanghai, China).
- [119] F. Zhou, et al., Subchondral trabecular microstructure and articular cartilage damage variations between osteoarthritis and osteoporotic osteoarthritis: a cross-sectional cohort study, *Front. Med.* 8 (2021) no pagination.
- [120] K. Chiba, et al., Relationship between microstructure and degree of mineralization in subchondral bone of osteoarthritis: a synchrotron radiation muCT study, *J. Bone Miner. Res.* 27 (7) (2012) 1511–1517.
- [121] S. Ajami, et al., Spatial links between subchondral bone architectural features and cartilage degeneration in osteoarthritic joints, *Sci. Rep.* 12 (1) (2022) 6694.
- [122] B.S. Baker, et al., Tibial bone quality in former bariatric surgery patients with osteoarthritis, *Obes. Surg.* 31 (12) (2021) 5322–5329.
- [123] T. Duvancic, et al., Novel micro-MRI approach for subchondral trabecular bone analysis in patients with hip osteoarthritis is comparable to micro-CT approach, *Croat. Med. J.* 63 (6) (2022) 515–524.
- [124] J. Kusins, et al., Full-field experimental analysis of the influence of microstructural parameters on the mechanical properties of humeral head trabecular bone, *J. Orthop. Res.* 40 (9) (2022) 2048–2056.
- [125] K. Liu, et al., Microstructural and histomorphological features of osteophytes in late-stage human knee osteoarthritis with varus deformity, *Joint Bone Spine* 89 (4) (2022), 105353.
- [126] D. Muratovic, et al., Elevated levels of active transforming growth factor beta1 in the subchondral bone relate spatially to cartilage loss and impaired bone quality in human knee osteoarthritis, *Osteoarthr. Cartil.* 30 (6) (2022) 896–907.
- [127] A. Nakasone, et al., Structural features of subchondral bone cysts and adjacent tissues in hip osteoarthritis, *Osteoarthr. Cartil.* 30 (8) (2022) 1130–1139.
- [128] T. Pascart, et al., Subchondral involvement in osteonecrosis of the femoral head: insight on local composition, microstructure and vascularization, *Osteoarthr. Cartil.* 30 (8) (2022) 1103–1115.
- [129] S. Taheri, et al., Changes of the subchondral bone microchannel network in early osteoarthritis, *Osteoarthr. Cartil.* 31 (1) (2023) 49–59.
- [130] J. Abbas, et al., Facet joints arthrosis in normal and stenotic lumbar spines, *Spine* 36 (24) (2011) E1541–E1546.
- [131] D. Abler, et al., A statistical shape model to predict the premorbid glenoid cavity, *J. Shoulder Elb. Surg.* 27 (10) (2018) 1800–1808.
- [132] S. de Raedt, et al., A three-dimensional analysis of osteoarthritic changes in the thumb carpometacarpal joint, *J. Hand Surg. Eur. Vol.* 38 (8) (2013) 851–859.
- [133] H. Aiba, et al., Radiographic analysis of subclinical appearances of the hip joint among patients with labral tears, *J. Orthop. Surg.* 14 (1) (2019) 369.
- [134] M. Asada, et al., Degeneration of the sacroiliac joint in hip osteoarthritis patients: a three-dimensional image analysis, *J. Belgian Soc. Radiol.* 103 (1) (2019) (no pagination).
- [135] P. Boileau, et al., Automated three-dimensional measurement of glenoid version and inclination in arthritic shoulders, *J. Bone Joint Surg. (Am. Vol.)* 100 (1) (2018) 57–65.
- [136] S. Bouacida, et al., Interest in the glenoid hull method for analyzing humeral subluxation in primary glenohumeral osteoarthritis, *J. Shoulder Elb. Surg.* 26 (7) (2017) 1128–1136.
- [137] K. Chiba, et al., In vivo structural analysis of subchondral trabecular bone in osteoarthritis of the hip using multi-detector row CT, *Osteoarthr. Cartil.* 19 (2) (2011) 180–185.
- [138] J.J. Crisco, et al., Osteophyte growth in early thumb carpometacarpal osteoarthritis, *Osteoarthr. Cartil.* 27 (9) (2019) 1315–1323.
- [139] Y. Ishii, et al., Size of medial knee osteophytes correlates with knee alignment but not with coronal laxity in patients with medial knee osteoarthritis, *J. Orthop. Res.* 38 (3) (2020) 639–644.
- [140] L. Kalichman, et al., Changes in paraspinal muscles and their association with low back pain and spinal degeneration: CT study, *Eur. Spine J.* 19 (7) (2010) 1136–1144.
- [141] L. Kalichman, et al., Computed tomography-evaluated features of spinal degeneration: prevalence, intercorrelation, and association with self-reported low back pain, *Spine J.* 10 (3) (2010) 200–208.
- [142] N.K. Knowles, et al., Regional bone density variations in osteoarthritic glenoids: a comparison of symmetric to asymmetric (type B2) erosion patterns, *J. Shoulder Elb. Surg.* 24 (3) (2015) 425–432.
- [143] N.K. Knowles, et al., Quantification of the position, orientation, and surface area of bone loss in type B2 glenoids, *J. Shoulder Elb. Surg.* 24 (4) (2015) 503–510.
- [144] S.H. Lee, et al., Diagnostic accuracy of low-dose versus ultra-low-dose CT for lumbar disc disease and facet joint osteoarthritis in patients with low back pain with MRI correlation, *Skelet. Radiol.* 47 (4) (2018) 491–504.
- [145] K. Liu, et al., The prevalence of osteoarthritis of the atlanto-odontoid joint in adults using multidetector computed tomography, *Acta Radiol. (Stockholm, Sweden)* 55 (1) (2014) 95–100.
- [146] A.F. Lombardi, et al., High-density mineralized protrusions and central osteophytes: associated osteochondral junction abnormalities in osteoarthritis, *Diagnostics* 10 (12) (2020) no pagination.
- [147] T. Nakasa, et al., Correlation between subchondral bone plate thickness and cartilage degeneration in osteoarthritis of the ankle, *Foot Ankle Int.* 35 (12) (2014) 1341–1349.
- [148] P. Omoumi, et al., Relationships between cartilage thickness and subchondral bone mineral density in non-osteoarthritic and severely osteoarthritic knees: in vivo concomitant 3D analysis using CT arthrography, *Osteoarthr. Cartil.* 27 (4) (2019) 621–629.
- [149] M.S. Sahin, A. Ergun, A. Aslan, The relationship between osteoarthritis of the lumbar facet joints and lumbosacropelvic morphology, *Spine* 40 (19) (2015) (p. E1058-62).
- [150] M.T.Y. Schneider, et al., Early morphologic changes in trapeziometacarpal joint bones with osteoarthritis, *Osteoarthr. Cartil.* 26 (10) (2018) 1338–1344.
- [151] J.J. Schreiber, et al., Changes in local bone density in early thumb carpometacarpal joint osteoarthritis, *J. Hand Surg.* 43 (1) (2018) 33–38.
- [152] Q. Song, et al., Evaluation of MRI and CT parameters to analyze the correlation between disc and facet joint degeneration in the lumbar three-joint complex, *Medicine* 98 (40) (2019), e17336.
- [153] P. Suri, et al., Presence and extent of severe facet joint osteoarthritis are associated with back pain in older adults, *Osteoarthr. Cartil.* 21 (9) (2013) 1199–1206.
- [154] P. Suri, et al., Does lumbar spinal degeneration begin with the anterior structures? A study of the observed epidemiology in a community-based population, *BMC Musculoskelet. Disord.* 12 (2011) 202 (Suri) Division of PM and R, VA Boston Healthcare System, Boston, United States.
- [155] P. Suri, et al., Vascular disease is associated with facet joint osteoarthritis, *Osteoarthr. Cartil.* 18 (9) (2010) 1127–1132.
- [156] E. Thienpont, P.-E. Schwab, P. Omoumi, Wear patterns in anteromedial osteoarthritis of the knee evaluated with CT-arthrography, *Knee* 21 (S1) (2014) S15–S19.
- [157] T.D. Turmezei, et al., A new CT grading system for hip osteoarthritis, *Osteoarthr. Cartil.* 22 (10) (2014) 1360–1366.
- [158] T. Turmezei, et al., Severity mapping of the proximal femur: a new method for assessing hip osteoarthritis with computed tomography, *Osteoarthr. Cartil.* 22 (10) (2014) 1488–1498.
- [159] Y. Yang, et al., Classification and morphological parameters of the calcaneal Talar facet: which type is more likely to cause osteoarthritis in Chinese population? *Biomed. Res. Int.* 2019 (2019) no pagination.
- [160] H. Alexander, et al., Atraumatic femoral head necrosis: a biomechanical, histological and radiological examination compared to primary hip osteoarthritis, *Arch. Orthop. Trauma Surg.* 142 (11) (2022) 3093–3099.



- [161] N.S. Alnusif, et al., Effectiveness of radiographs and computed tomography in evaluating primary elbow osteoarthritis, *J. Shoulder Elb. Surg.* 30 (7S) (2021) S8–S13.
- [162] C.J. Burke, et al., Ultrasound and PET-CT correlation in shoulder pathology: a 5-year retrospective analysis, *Clin. Nucl. Med.* 42 (10) (2017) e424–e430.
- [163] R. Carr, et al., Four-dimensional computed tomography scanning for dynamic wrist disorders: prospective analysis and recommendations for clinical utility, *J. Wrist Surg.* 8 (2) (2019) 161–167.
- [164] C. Egloff, et al., Changes of density distribution of the subchondral bone plate after supramalleolar osteotomy for valgus ankle osteoarthritis, *J. Orthop. Res.* 32 (10) (2014) 1356–1361.
- [165] A.S. Ha, et al., Weightbearing digital Tomosynthesis of foot and ankle arthritis: comparison with radiography and simulated Weightbearing CT in a prospective study, *AJR Am. J. Roentgenol.* 212 (1) (2019) 173–179.
- [166] Y.H. Hong, E.J. Kong, (18F)Fluoro-deoxy-D-glucose uptake of knee joints in the aspect of age-related osteoarthritis: a case-control study, *BMC Musculoskelet. Disord.* 14 (2013) 141.
- [167] F. Intema, et al., Subchondral bone remodeling is related to clinical improvement after joint distraction in the treatment of ankle osteoarthritis, *Osteoarthr. Cartil.* 19 (6) (2011) 668–675.
- [168] L. Kalichman, et al., Indices of paraspinal muscles degeneration: reliability and association with facet joint osteoarthritis: feasibility study, *Clin. Spine Surg.* 29 (9) (2016) 465–470.
- [169] S. Kitanaka, et al., Facet joint osteoarthritis affects spinal segmental motion in degenerative spondylolisthesis, *Clin. Spine Surg.* 31 (8) (2018) E386–E390.
- [170] T. Lowitz, et al., Bone marrow lesions identified by MRI in knee osteoarthritis are associated with locally increased bone mineral density measured by QCT, *Osteoarthr. Cartil.* 21 (7) (2013) 957–964.
- [171] J.T. Lynch, et al., Statistical shape modelling reveals large and distinct subchondral bony differences in osteoarthritic knees, *J. Biomech.* 93 (2019) 177–184.
- [172] F. Massilla Mani, S.S. Sivasubramanian, A study of temporomandibular joint osteoarthritis using computed tomographic imaging, *Biom. J.* 39 (3) (2016) 201–206.
- [173] A.-A. Najefi, Y. Ghani, A.J. Goldberg, Bone cysts and osteolysis in ankle replacement, *Foot Ankle Int.* 42 (1) (2021) 55–61.
- [174] D.D. Nowak, et al., Interobserver and intraobserver reliability of the Walch classification in primary glenohumeral arthritis, *J. Shoulder Elb. Surg.* 19 (2) (2010) 180–183.
- [175] H. Seki, et al., Visualization and quantification of the degenerative pattern of the talus in unilateral varus ankle osteoarthritis, *Sci. Rep.* 9 (1) (2019) 17438.
- [176] M. Sugano, et al., Comparison study of bone strength of the proximal femur with and without hip osteoarthritis by computed tomography-based finite element analysis, *J. Biomech.* 105 (2020), 109810.
- [177] W.N. Zeng, et al., Investigation of association between hip morphology and prevalence of osteoarthritis, *Sci. Rep.* 6 (2016) 23477.
- [178] J. Chen, et al., Tibial tubercle-Roman arch (TT-RA) distance is superior to tibial tubercle-trochlear groove (TT-TG) distance when evaluating coronal malalignment in patients with knee osteoarthritis, *Eur. Radiol.* 32 (12) (2022) 8404–8413.
- [179] X.-H. Dong, et al., Three-dimensional morphometric differences of resected distal femurs and proximal tibias in osteoarthritic and normal knees, *BMC Musculoskelet. Disord.* 22 (1) (2021) 1013.
- [180] A. Haj-Mirzaian, et al., Kinematic tibiofibular syndesmotomic measurements as indicators of tibiotalar osteoarthritis: exploratory analysis using 4-dimensional computed tomography, *J. Comput. Assist. Tomogr.* 46 (4) (2022) 633–637.
- [181] S.W. Hong, J.-H. Kang, Bone mineral density, bone microstructure, and bone turnover markers in females with temporomandibular joint osteoarthritis, *Clin. Oral Investig.* 25 (11) (2021) 6435–6448.
- [182] G. Jiang, J. Ding, C. Ge, Deep learning-based CT imaging to evaluate the therapeutic effects of acupuncture and moxibustion therapy on knee osteoarthritis, *Comput. Math. Methods Med.* 2022 (2022) 1135196.
- [183] A.M. Morton, et al., Bone morphological changes of the trapezium and first metacarpal with early thumb osteoarthritis progression, *Clin. Biomech. (Bristol, Avon)* 100 (2022), 105791.
- [184] P. Omoumi, et al., Proximal tibial osteophyte volumes are correlated spatially and with knee alignment: a quantitative analysis suggesting the influence of biochemical and mechanical factors in the development of osteophytes, *Osteoarthr. Cartil.* 29 (12) (2021) 1691–1700.
- [185] H. Seki, et al., Visualization and quantification of the degenerative pattern of the distal tibia and fibula in unilateral varus ankle osteoarthritis, *Sci. Rep.* 11 (1) (2021) 21628.
- [186] N. Serrano, et al., CT-based and morphological comparison of glenoid inclination and version angles and mineralisation distribution in human body donors, *BMC Musculoskelet. Disord.* 22 (1) (2021) 849.
- [187] Y. Suga, et al., Factors associated with the increased risk of atlantoaxial osteoarthritis: a retrospective study, *Eur. Spine J.* 31 (12) (2022) 3418–3425.
- [188] A.K. Abrahamsson, et al., Frequency of temporomandibular joint osteoarthritis and related symptoms in a hand osteoarthritis cohort, *Osteoarthr. Cartil.* 25 (5) (2017) 654–657.
- [189] A.A. Almashraqi, et al., Cone beam computed tomography findings in temporomandibular joint of chronic qat chewers: dimensional and osteoarthritic changes, *J. Oral Rehabil.* 47 (12) (2020) 1538–1549.
- [190] R. Arayasantiparb, et al., Association of radiographic and clinical findings in patients with temporomandibular joints osseous alteration, *Clin. Oral Investig.* 24 (1) (2020) 221–227.
- [191] M. Bakke, et al., Bony deviations revealed by cone beam computed tomography of the temporomandibular joint in subjects without ongoing pain, *J. Oral Facial Pain Headache* 28 (4) (2014) 331–337.
- [192] M.O. Borahan, M. Mayil, F.N. Pekiner, Using cone beam computed tomography to examine the prevalence of condylar bony changes in a Turkish subpopulation, *Niger. J. Clin. Pract.* 19 (2) (2016) 259–266.
- [193] L.H. Cevidanes, et al., 3D superimposition and understanding temporomandibular joint arthritis, *Orthod. Craniofacial Res.* 18 (Suppl. 1) (2015) 18–28.
- [194] L.H. Cevidanes, et al., Quantification of condylar resorption in temporomandibular joint osteoarthritis, *Oral Surg. Oral Med. Oral Pathol. Oral Radiol. Endod.* 110 (1) (2010) 110–117.
- [195] L.H. Cevidanes, et al., 3D osteoarthritic changes in TMJ condylar morphology correlates with specific systemic and local biomarkers of disease, *Osteoarthr. Cartil.* 22 (10) (2014) 1657–1667.
- [196] S. Chen, et al., Cephalometric analysis of the facial skeletal morphology of female patients exhibiting skeletal class II deformity with and without temporomandibular joint Osteoarthritis, *PLoS One* 10 (10) (2015), e0139743.
- [197] L.R. Gomes, et al., Diagnostic index of three-dimensional osteoarthritic changes in temporomandibular joint condylar morphology, *J. Med. Imaging* 2 (3) (2015) (no pagination).
- [198] D. Ilguy, et al., Articular eminence inclination, height, and condyle morphology on cone beam computed tomography, *Sci. World J.* 2014 (2014) (no pagination).
- [199] S. Kayipmaz, et al., Trabecular structural changes in the mandibular condyle caused by degenerative osteoarthritis: a comparative study by cone-beam computed tomography imaging, *Oral Radiol.* 35 (1) (2019) 51–58.
- [200] P. Kvarda, et al., 3D assessment in posttraumatic ankle osteoarthritis, *Foot Ankle Int.* 42 (2) (2021) 200–214.
- [201] P.P. Lee, A.R. Stanton, L.G. Hollender, Greater mandibular horizontal condylar angle is associated with temporomandibular joint osteoarthritis, *Oral Surg Oral Med Oral Pathol Oral Radiol* 123 (4) (2017) 502–507.
- [202] X. Liang, et al., Evaluation of trabecular structure changes in osteoarthritis of the temporomandibular joint with cone beam computed tomography imaging, *Oral Surg Oral Med Oral Pathol Oral Radiol* 124 (3) (2017) 315–322.
- [203] K.A. Myller, et al., In vivo contrast-enhanced cone beam CT provides quantitative information on articular cartilage and subchondral bone, *Ann. Biomed. Eng.* 45 (3) (2017) 811–818.
- [204] S.M. Ok, et al., Anterior condylar remodeling observed in stabilization splint therapy for temporomandibular joint osteoarthritis, *Oral Surg. Oral Med. Oral Pathol. Oral Radiol.* 118 (3) (2014) 363–370.
- [205] M.K. Ottersen, et al., CBCT characteristics and interpretation challenges of temporomandibular joint osteoarthritis in a hand osteoarthritis cohort, *Dentomaxillofac. Radiol.* 48 (4) (2019) 20180245.
- [206] J. Shi, et al., Association of condylar bone quality with TMJ osteoarthritis, *J. Dent. Res.* 96 (8) (2017) 888–894.
- [207] D. Soydan, et al., Effect of internal derangements and degenerative bone changes on the minimum thickness of the roof of the glenoid fossa in temporomandibular joint, *Oral Radiol.* 36 (1) (2020) 25–31.
- [208] H. Sun, et al., Clinical outcome of sodium hyaluronate injection into the superior and inferior joint space for osteoarthritis of the temporomandibular joint evaluated by cone-beam computed tomography: a retrospective study of 51 patients and 56 joints, *Med. Sci. Monit.* 24 (dxw, 9609063) (2018) 5793–5801.
- [209] J.B. Drihan, et al., Validation of quantitative magnetic resonance imaging-based apparent bone volume fraction in peri-articular tibial bone of cadaveric knees, *BMC Musculoskelet. Disord.* 15 (100968565) (2014) 143.
- [210] J.B. Renault, et al., Tibial subchondral trabecular bone micromechanical and microarchitectural properties are affected by alignment and osteoarthritis stage, *Sci. Rep.* 10 (1) (2020) 3975.
- [211] N.A. Segal, et al., Diagnostic performance of 3D standing CT imaging for detection of knee osteoarthritis features, *Phys. Sportsmed.* 43 (3) (2015) 213–220.
- [212] J. Steadman, et al., Comparative assessment of midfoot osteoarthritis diagnostic sensitivity using weightbearing computed tomography vs weightbearing plain radiography, *Eur. J. Radiol.* 134 (2021), 109419.
- [213] J. Bianchi, et al., Quantitative bone imaging biomarkers to diagnose temporomandibular joint osteoarthritis, *Int. J. Oral Maxillofac. Surg.* 50 (2) (2021) 227–235.
- [214] J. Bianchi, et al., Radiographic interpretation using high-resolution Cbct to diagnose degenerative temporomandibular joint disease, *PLoS One* 16 (8) (2021), e0255937.
- [215] E. Choi, et al., Artificial intelligence in detecting temporomandibular joint osteoarthritis on orthopantomogram, *Sci. Rep.* 11 (1) (2021) 10246.
- [216] K. Han, et al., A long-term longitudinal study of the osteoarthritic changes to the temporomandibular joint evaluated using a novel three-dimensional superimposition method, *Sci. Rep.* 11 (1) (2021) 9389.
- [217] H.W. Kang, et al., Coronal plane calcaneal-Talar orientation in Varus ankle osteoarthritis, *Foot Ankle Int.* 43 (7) (2022) 928–936.
- [218] M.T. Nevalainen, M.-M. Pitkanen, S. Saarakkala, Diagnostic performance of ultrasonography for evaluation of osteoarthritis of ankle joint: comparison with radiography, cone-beam CT, and symptoms, *J. Ultrasound Med.* 41 (5) (2022) 1139–1146.
- [219] U. Pamukcu, et al., Does the horizontal condylar angle have a relationship to temporomandibular joint osteoarthritis and condylar position? A cone-beam computed tomography study, *Folia Morphol. (Warsz)* 81 (3) (2022) 723–731.
- [220] N.A. Segal, et al., Clinical value of weight-bearing CT and radiographs for detecting patellofemoral cartilage visualized by MRI in the MOST study, *Osteoarthr. Cartil.* 29 (11) (2021) 1540–1548.

- [221] M. Amini, et al., Individual and combined effects of OA-related subchondral bone alterations on proximal tibial surface stiffness: a parametric finite element modeling study, *Med. Eng. Phys.* 37 (8) (2015) 783–791.
- [222] W.D. Burnett, et al., Knee osteoarthritis patients with more subchondral cysts have altered tibial subchondral bone mineral density, *BMC Musculoskelet. Disord.* 20 (1) (2019) 14.
- [223] W.D. Burnett, et al., Regional depth-specific subchondral bone density measures in osteoarthritic and normal patellae: in vivo precision and preliminary comparisons, *Osteoporos. Int.* 25 (3) (2014) 1107–1114.
- [224] J.D. Johnston, et al., A comparison of conventional maximum intensity projection with a new depth-specific topographic mapping technique in the CT analysis of proximal tibial subchondral bone density, *Skelet. Radiol.* 39 (9) (2010) 867–876.
- [225] J.D. Johnston, et al., In vivo precision of a depth-specific topographic mapping technique in the CT analysis of osteoarthritic and normal proximal tibial subchondral bone density, *Skelet. Radiol.* 40 (8) (2011) 1057–1064.
- [226] J.-W. Lee, A. Kobayashi, T. Nakano, Crystallographic orientation of the c-axis of biological apatite as a new index of the quality of subchondral bone in knee joint osteoarthritis, *J. Bone Miner. Metab.* 35 (3) (2017) 308–314.
- [227] F. Sannmann, et al., Impact of meniscal coverage on subchondral bone mineral density of the proximal tibia in female subjects - a cross-sectional in vivo study using QCT, *Bone* 134 (2020) 115292 (Sannmann, Engelke) Institute of Medical Physics, University of Erlangen-Nurnberg, Henkestr 91, Erlangen 91052, Germany.
- [228] J.L. Bhatla, et al., Differences in subchondral bone plate and cartilage thickness between women with anterior cruciate ligament reconstructions and uninjured controls, *Osteoarthr. Cartil.* 26 (7) (2018) 929–939.
- [229] K. Chiba, et al., Three-dimensional analysis of subchondral cysts in hip osteoarthritis: an ex vivo HR-pQCT study, *Bone* 66 (asr, 8504048) (2014) 140–145.
- [230] M.H. Edwards, et al., The relationship of bone properties using high resolution peripheral quantitative computed tomography to radiographic components of hip osteoarthritis, *Osteoarthr. Cartil.* 25 (9) (2017) 1478–1483.
- [231] S. Finzel, et al., Inflammatory bone spur formation in psoriatic arthritis is different from bone spur formation in hand osteoarthritis, *Arthritis Rheum.* 66 (11) (2014) 2968–2975.
- [232] K. Shiraishi, et al., In vivo analysis of subchondral trabecular bone in patients with osteoarthritis of the knee using second-generation high-resolution peripheral quantitative computed tomography (HR-pQCT), *Bone* 132 (2020) 115155 (Shiraishi, Chiba, Okazaki, Yokota, Nakazoe, Kidera, Yonekura, Tomita, Osaki) Department of Orthopedic Surgery, Nagasaki University Graduate School of Biomedical Sciences, Nagasaki, Japan.
- [233] T. Turmezei, et al., A new CT grading system for hip osteoarthritis, *Osteoarthr. Cartil.* 22 (10) (2014) 1360–1366.
- [234] W.D. Burnett, et al., Knee osteoarthritis patients with severe nocturnal pain have altered proximal tibial subchondral bone mineral density, *Osteoarthr. Cartil.* 23 (9) (2015) 1483–1490.
- [235] Paul Scherrer Institute (PSI), TOMCAT - X02DA: Tomographic Microscopy: A Beamline for TOMographic Microscopy and Coherent rAdiology experiments, Paul Scherrer Institut PSI, 2023 cited 28 September, <https://www.psi.ch/en/sls/tomcat>.
- [236] ANSTO, Micro-Computed Tomography beamline (MCT), ANSTO, 2023 [cited 28 September 2023], <https://www.ansto.gov.au/micro-computed-tomography-beamline#content-technical-information>.
- [237] J.-P. Grunz, et al., Image quality assessment for clinical cadmium telluride-based photon-counting computed tomography detector in cadaveric wrist imaging, *Investig. Radiol.* 56 (12) (2021) 785–790.
- [238] N. Kämmerling, et al., Assessment of image quality in photon-counting detector computed tomography of the wrist—an ex vivo study, *Eur. J. Radiol.* 154 (2022), 110442.
- [239] F.S.L. Thomsen, et al., Effective spatial resolution of photon counting CT for imaging of trabecular structures is superior to conventional clinical CT and similar to high resolution peripheral CT, *Investig. Radiol.* 57 (9) (2022) 620–626.
- [240] C. Chappard, et al., Virtual monoenergetic images from photon-counting spectral computed tomography to assess knee osteoarthritis, *Eur. Radiol. Exp.* 6 (1) (2022) 1–10.
- [241] M. Kalladka, et al., Temporomandibular joint osteoarthritis: diagnosis and long-term conservative management: a topic review, *J. Indian Prosthodont. Soc.* 14 (1) (2014) 6–15.
- [242] K.-S. Nah, Condylar bony changes in patients with temporomandibular disorders: a CBCT study, *Imaging Sci. Dent.* 42 (4) (2012) 249–253.
- [243] T. Eckersley, J. Faulkner, O. Al-Dadah, Inter- and intra-observer reliability of radiological grading systems for knee osteoarthritis, *Skelet. Radiol.* 50 (2021) 2069–2078.
- [244] H.K. Genant, et al., Quantitative computed tomography in assessment of osteoporosis, in: *Seminars in Nuclear Medicine*, Elsevier, 1987.
- [245] S.Y. Lee, et al., Reliability and validity of lower extremity computed tomography as a screening tool for osteoporosis, *Osteoporos. Int.* 26 (4) (2015) 1387–1394.
- [246] P.J. Pickhardt, et al., Opportunistic screening for osteoporosis using abdominal computed tomography scans obtained for other indications, *Ann. Intern. Med.* 158 (8) (2013) 588–595.
- [247] M.T. Hannan, et al., Bone mineral density and knee osteoarthritis in elderly men and women. The Framingham study, *Arthritis Rheum.* 36 (12) (1993) 1671–1680.
- [248] M.C. Nevitt, et al., Radiographic osteoarthritis of the hip and bone mineral density, *Arthritis Rheum.* 38 (7) (1995) 907–916.
- [249] N.A. Segal, et al., Test–retest reliability of tibiofemoral joint space width measurements made using a low-dose standing CT scanner, *Skelet. Radiol.* 46 (2) (2017) 217–222.
- [250] N.A. Segal, et al., Comparison of tibiofemoral joint space width measurements from standing CT and fixed flexion radiography, *J. Orthop. Res.* 35 (7) (2017) 1388–1395.
- [251] T. Turmezei, et al., Quantitative Three-dimensional Assessment of Knee Joint Space Width From Weight-bearing CT, 2021.
- [252] T.D. Turmezei, et al., Multiparametric 3-D analysis of bone and joint space width at the knee from weight bearing computed tomography, *Osteoarthr. Imaging* 2 (2) (2022), 100069.
- [253] T.D. Turmezei, et al., Quantitative 3D imaging parameters improve prediction of hip osteoarthritis outcome, *Sci. Rep.* 10 (1) (2020) 4127.
- [254] P. Omoumi, et al., CT arthrography, MR arthrography, PET, and scintigraphy in osteoarthritis, *Radiol. Clin.* 47 (4) (2009) 595–615.
- [255] P. Omoumi, et al., Diagnostic performance of CT-arthrography and 1.5 T MR-arthrography for the assessment of glenohumeral joint cartilage: a comparative study with arthroscopic correlation, *Eur. Radiol.* 25 (4) (2015) 961–969.
- [256] A. Wyler, et al., Hyaline cartilage thickness in radiographically normal cadaveric hips: comparison of spiral CT arthrographic and macroscopic measurements, *Radiology* 242 (2) (2007) 441–449.